Universidade do Minho
Escola de Ciências da Saúde

Sofia Pereira das Neves

STUDYING THE ROLE OF LIPOCALIN-2 IN THE PATHOPHYSIOLOGY OF MULTIPLE SCLEROSIS – LOOKING BEYOND THE BRAIN

O PAPEL DA LIPOCALIN-2 NA PATOFISIOLOGIA DA ESCLEROSE MÚLTIPLA – UM OLHAR PARA ALÉM DO CÉREBRO

Maio 2015

Universidade do Minho
Escola de Ciências da Saúde

Sofia Pereira das Neves

STUDYING THE ROLE OF LIPOCALIN-2 IN THE PATHOPHYSIOLOGY OF MULTIPLE SCLEROSIS – LOOKING BEYOND THE BRAIN

O PAPEL DA LIPOCALIN-2 NA PATOFISIOLOGIA DA ESCLEROSE MÚLTIPLA – UM OLHAR PARA ALÉM DO CÉREBRO

Dissertação de Mestrado
Mestrado em Ciências da Saúde

Trabalho realizado sob a orientação de
Professora Doutora Fernanda Marques
e do
Professor Doutor João José Cerqueira

Maio 2015

Nome: Sofia Pereira das Neves

Endereço eletrónico: sofianeves@ecsaude.uminho.pt Telefone: 913372844

Bilhete de Identidade/Cartão do Cidadão: 13364864

Título da dissertação: Studying the role of lipocalin-2 in the pathophysiology of multiple sclerosis – Looking beyond the brain

Orientadores:

Professora doutora Fernanda Marques

Professor doutor João José Cerqueira

Ano de conclusão: 2015

Mestrado em Ciências da Saúde

É AUTORIZADA A REPRODUÇÃO INTEGRAL DESTA DISSERTAÇÃO APENAS PARA EFEITOS DE INVESTIGAÇÃO, MEDIANTE DECLARAÇÃO ESCRITA DO INTERESSADO, QUE A TAL SE COMPROMETE.

Universidade do Minho, _____/_____/_____

Assinatura:

Para a Carla e para o Ricardo

AGRADECIMENTOS

A presente dissertação de mestrado resulta do trabalho que desenvolvi no ICVS, mas nunca poderia ter sido feita sem a ajuda de todos aqueles a quem passo a agradecer. Para quem me conhece sabe que eu não sou de grandes discursos, daí que os meus agradecimentos possam parecer pobres, mas saibam que valorizo muito todos os mencionados.

À Fernanda, uma grande orientadora, que esteve sempre presente para me ensinar e para me ajudar sempre que alguma coisa não corria tão bem, tanto a nível profissional como pessoal. Também me deu os merecidos raspanetes, que me ajudaram a melhorar o meu método de trabalho, e a tentar relativizar mais as coisas. Obrigado!

Ao João, pelas sugestões e ajuda, e por ter apostado em mim e me ter dado a minha primeira oportunidade de trabalho, o que me permitiu continuar no ICVS e percorrer todo este longo caminho.

Aos meus amiguinhos de grupo, a Catarina e o Sandro, que tiveram a paciência para partilhar comigo os seus conhecimentos, que estiveram presentes para me ajudar, e tiveram uma palavra de carinho, sempre que precisei.

À Cláudia Miranda, pelo imenso apoio que me deu numa área da qual eu sabia muito pouco.

Ao Nuno Sousa, à Margarida Correia-Neves e à Joana Palha, pelas discussões científicas e sugestões dadas.

À Susana Roque, ao Bruno e à Cláudia Nobrega, pela ajuda com a parte imunológica do trabalho.

A todos os membros do restante grupo, Ashley, João Sousa, João Costa, Leonor, Diana e Ana pelas sugestões em todas as reuniões.

À Sónia Gomes por sermos as umas choramingas que se apoiam uma à outra. Serás sempre a minha companheira de cativeiro.

À Gabriela e ao restante astrogang pela ajuda com a parte dos astrócitos.

À Cristina e à Susana Monteiro, por serem boas companheiras de meu 2º grupo.

Às minhas companheiras de almoço, a Fátima Lopes, a Liliana e a Sónia Borges.

A todos aqueles que foram em busca de novos desafios longe de Braga, mas que deixaram a sua marca: Ana Oliveira, Sara, Daniela, Filipa, Filipe

Às restantes companheiras do I201, sempre as mais animadas: Dulce, Fátima Ramalhosa, Rita, Cláudia Antunes, Vanessa, Neide, Marta, Francisca. E Eduardo, o homem no meio das mulheres.

À minha amiga para a vida, Diana, que também esteve sempre disponível para discutir comigo e ouvir-me.

A todos os meus amigos, da terrinha ou antigos colegas de curso. Aprendi algo com todos vocês.

Aos meus companheiros de mestrado, que partilharam alguns dos meus problemas e angústias, principalmente à minha colega da frente, a Isabel, com quem convivi vários vezes fora do horário de trabalho.

A todos os NERD's, pelo ambiente de trabalho que criaram e me faz querer continuar cá.

Por fim, às 4 pessoas mais importantes da minha vida: a minha irmã Carla e o meu namorado Ricardo, que sempre acreditaram em mim e nas minhas capacidades, mesmo quando eu própria não acreditava; e aos meus grandes PAIS, porque sem eles eu não estaria aqui, e por todos os sacrifícios que fizeram desde sempre.

Esta tese de mestrado decorreu no âmbito do projeto financiado pela Fundação para a Ciência e Tecnologia (FCT) e COMPETE através do projeto EXPL/NEU-OSD/2196/2013.

Studying the Role of Lipocalin-2 in the Pathophysiology of Multiple Sclerosis – Looking beyond the brain

ABSTRACT

Multiple sclerosis (MS) is an immune-mediated demyelinating disease of the central nervous system (CNS), characterized by the presence of demyelination plaques, inflammation and gliosis that consequently lead to axonal damage. The sequence of events that leads to demyelination remains unclear and the pathophysiological mechanisms are diverse. Also, although this is a disease of the CNS, there is no doubt that, in terms of peripheral organs, the thymus, as the organ of T cell differentiation and maturation, plays an important role in the pathophysiology of the disease.

Recently, the levels of lipocalin 2 (LCN2), an acute phase protein that is part of the defense system against bacteria, by binding to iron-loaded siderophores, were found to be increased in cerebrospinal fluid (CSF) and serum of MS patients, when compared to control subjects. Similarly, using the MS animal model of experimental autoimmune encephalomyelitis (EAE), LCN2 was detected in brain parenchyma astrocytes, in regions typically affected in MS patients. This expression by astrocytes, together with an increased LCN2 level in the CSF, occurs during the active phases of the disease, which could point towards a role for LCN2 secreted by astrocytes in the mediation of inflammatory responses in the EAE model. Altogether, these findings support LCN2 as a valuable molecule for the diagnostic/monitoring of MS and suggest its potential involvement as a disease modulator. Of relevance, the exact role of LCN2 in the pathophysiology of the disease remains largely unknown and contradictory data exists on its potential protective or deleterious effect. Therefore, we sought to investigate the role of LCN2 in the onset and progression of the disease. Herein, we tackled the disease, by evaluating the role of LCN2, not only in the perspective of the CNS, but also on the perspective of peripheral organs such as the thymus.

First we intended to perform a characterization of the thymus regarding thymocyte populations and histological morphology, in wild-type (WT) animals induced with EAE, in the onset and chronic phases of disease. Next, to further understand the role of LCN2 in MS pathology, we induced EAE both in LCN2-null mice and in WT littermates. Non-induced EAE animals were used as controls.

The thymus of EAE animals was atrophied, as assessed by its weight, normalized for total body weight, and by the number of total cells. Also, we found a decrease in total cell number of all thymocyte populations, during the onset and chronic phases of EAE. In relative terms, the percentage of double positive cells was decreased, and the percentages of the cluster of differentiation (CD)4 and CD8 single positive cells were increased, during the onset phase. At the chronic phase, the proportions between the different populations were restored.

LCN2-null mice induced with EAE did not present major alterations in terms of the clinical score, when compared with WT littermates also induced with EAE. Likewise, their thymic alterations were similar to the ones observed in WT EAE animals. Of relevance, as for the inflammatory profile in the cerebellum, LCN2-null mice presented less inflammation, as assessed by decreased expression levels of pro-inflammatory cytokines interferon (*Ifn*)*-gamma*, interleukin (*Il*)12a and *Il17a*. Also of interest, the cerebellum of LCN2-null mice presented a decrease in the percentage of lesioned areas. Finally, EAE animals, from both genotypes, presented an increase in the area positive for glial fibrillary acidic protein (GFAP), in the white matter of the cerebellum, in both the onset and chronic phases of disease. On the contrary, the expression levels of *Gfap* in the cerebellum were only increased at the onset phase of disease.

KEYWORDS: MULTIPLE SCLEROSIS, LIPOCALIN-2, NEUROINFLAMMATION, ASTROCYTES, THYMUS, EXPERIMENTAL AUTOIMMUNE ENCEPHALOMYELITIS

O papel da lipocalin-2 na patofisiologia da Esclerose Múltipla – Um olhar para além do cérebro

RESUMO

A Esclerose Múltipla (EM) é uma doença autoimune desmielinizante do sistema nervosa central (SNC), caracterizada pela presença de placas de desmielinização, inflamação e gliose, que tem como consequência dano axonal. A sequência de eventos que induzem desmielinização permanecem desconhecidos, e os mecanismos patofisiológicos são diversos. Embora esta seja uma doença do SNC, não há dúvidas que, em termos de órgãos periféricos, o timo, sendo o órgão de maturação e diferenciação das células T, desempenha um papel importante na patofisiologia da doença.

Recentemente, os níveis de lipocalin-2 (LCN2), uma proteína de fase aguda que participa no sistema de defesa contra infeções bacterianas, através da ligação a sideróforos, foram encontrados como estando elevados no líquido cefalorraquidiano (LCR) e no soro de doentes com EM, comparativamente aos controlos. Da mesma maneira, usando o modelo animal de EM de encefalomielite autoimune experimental (EAE), a LCN2 foi detetada em astrócitos do parênquima, em regiões tipicamente afetadas em doentes com EM. Esta expressão pelos astrócitos, associada a um aumento de LCN2 no LCR, ocorreu durante as fases ativas da doença, o que aponta para um papel da LCN2 secretada pelos astrócitos na mediação da response inflamatória no modelo de EAE. No seu conjunto, estas evidências suportam o papel da LCN2 como uma molécula importante no diagnóstico e/ou monitorização da EM, e sugere o seu possível envolvimento como moduladora da doença. É relevante dizer que o papel exato da LCN2 na patofisiologia da doença permanece desconhecido, e existem dados contraditórios no que diz respeito ao seu potencial efeito protetor ou deletério. Por isso, nós procurámos perceber o papel da LCN2 no *onset* e na progressão da doença. Assim, nós investigámos o papel da LCN2 na doença, não só na perspetiva do SNC, mas também dos órgãos periféricos, nomeadamente do timo.

Primeiro pretendemos caracterizar o timo em relação às populações de timócitos e morfologia histológica, em animais *wild-type* (WT) induzidos com EAE, no *onset* e na fase crónica da doença. De seguida, para melhor entender o papel da LCN2 na patologia da EM, induzimos EAE em animais LCN2-*null* e em WT da mesma ninhada. Para além disso, usámos animais não induzidos como controlos.

Nós observámos que o timo dos animais induzidos com EAE estava atrofiado, com base no seu peso, após normalização para o peso total do animal, e no número total de células. Para além disso, encontrámos uma diminuição no número total de células de todas as principais populações de timócitos, durante o *onset* e fase crónica da doença. No que diz respeito à percentagem de cada uma das populações de timócitos, durante o *onset* da doença, a percentagem de células duplas positivas encontrava-se diminuída, enquanto as percentagens das populações CD4+CD8- e CD4-CD8+ se encontrava aumentada. Na fase crónica da doença, as proporções entre as diferentes populações foram reestabelecidas.

Os animais LCN2-*null* induzidos com EAE não apresentaram grandes alterações em termos de score clínico, quando comparados com os animais WT da mesma ninhada também induzidos com EAE. Para além disso, as alterações observadas no timo foram semelhantes às encontradas nos animais WT EAE. De relevância, no que diz respeito ao perfil inflamatório no cerebelo, os animais LCN2-*null* apresentaram menos inflamação, o que é suportado por níveis diminuídos dos níveis de expressão das citoquinas pró-inflamatórias interferão-gama, e interleucinas 12 e 17. É importante também referir que os cerebelos de animais LCN2-*null* apresentaram uma diminuição na percentagem de áreas com lesões. Os animais EAE, de ambos os genótipos, apresentaram um aumento na área positiva para GFAP, na substância branca do cerebelo, no *onset* e na fase crónica da doença. Pelo contrário, os níveis de expressão de *Gfap* no cerebelo só foram encontrados elevados no *onset da doença.*

PALAVRAS-CHAVE: ESCLEROSE MÚLTIPLA, LIPOCALINA-2, NEUROINFLAMAÇÃO, ASTRÓCITOS, TIMO, ENCEFALOMIELITE AUTOIMUNE EXPERIMENTAL

INDEX

Agradecimentos vi
Abstract ix
Resumo xi
Abbreviations and acronyms list xiv
Figures list xvi
Tables list xvii
1. Introduction 1
1.1 Multiple Sclerosis 2
1.2 Etiology of MS disease 3
1.3 MS symptoms 6
1.4 MS animal models – Experimental autoimmune encephalomyelitis 6
1.5 The role of glial cells in EAE 10
1.5.1 Oligodendrocytes 10
1.5.2 Microglia 11
1.5.3 Astrocytes 12
1.6 Lipocalin-2 13
1.6.1 Lipocalin-2 and CNS 14
1.6.2 Lipocalin-2 and MS 15
1.7 Role of the thymus in MS and EAE development 16
1.8 Research objectives 19
2. Experimental procedures 21
2.1 Mice 22
2.1.1 Genotyping 22
2.1.2 EAE induction 24
2.1.3 Sample collection 25
2.2 Flow cytometry 26
2.3 Gene expression analysis 27
2.4 Histological analysis 29
2.4.1 Thymic morphology 29
2.4.2 Immunofluorescence for GFAP 29
2.4.3 Luxol Fast Blue 30

2.5 Serum corticosterone quantification 30
2.6 Statistical analysis 31
3. Results 33
3.1 Chronic disease course in MOG_{35-55} induced EAE 34
3.2 The proportion of the four main populations of the thymus was altered in WT animals during the onset phase EAE but was restored in the chronic phase of disease 34
3.2.1 Corticosteroid measurement 37
3.3 Thymic histological morphology was altered in WT EAE animals 37
3.4 Disease course in LCN2-null mice was similar to WT animals 38
3.5 LCN2-null mice presented similar alterations to the WT animals regarding thymic populations, during EAE development 39
3.5.1 Corticosteroid measurements 42
3.6 LCN2 deficiency results in a decreased inflammatory profile in the cerebellum of EAE animals 43
3.6.1 Inflammatory cytokines expression levels 43
3.6.2 Inflammatory infiltrates in the cerebellum white matter 45
3.7 Astrogliosis is increased in the cerebellum during EAE 47
4. Discussion 49
4.1 Thymus characterization in the context of a chronic EAE model 50
4.1.1 Influence of the hypothalamic-pituitary-adrenal (HPA) axis in thymic alterations in the EAE animal model induced in WT 52
4.1.2 Histological alterations in the thymus 53
4.2 Role of LCN2 in the pathophysiology of EAE 53
4.2.1 Disease development in LCN2-null mice 53
4.2.2 Thymus alterations and the HPA axis in LCN2-null mice 55
4.2.3 Inflammation in the cerebellum 56
4.2.4 Astrogliosis in the cerebellum 58
5. Concluding remarks 59
6. References 63
Annex I – DNA sequences of the primers used in qRT-PCR 74

ABBREVIATIONS AND ACRONYMS LIST

2,5-DHBA - 2,5-dihydroxybenzoic acid
7-ADD – 7-Aminoactinomycin D
μL – Microliter

A
APC – Antigen presenting cell

B
BBB – Blood-brain barrier
Bcl-2 – B cell lymphoma 2
BIM – Bcl-2 interacting mediator of cell death

C
CD – Cluster of differentiation
cDNA – Complementary deoxyribonucleic acid
CFA – Freund's complete adjuvant
CIS – Clinically isolated syndrome
CNPase – 2',3'-cyclic-nucleotide 3'-phosphodiesterase
CNS – Central nervous system
CP – Choroid plexus
CSF – Cerebrospinal fluid

D
DAPI – 4', 6-diamino-2-phenylindole
DMEM – Dulbecco's modified eagle's medium
DN – Double negative
DNA – Deoxyribonucleic acid
DP – Double positive

E
EAE – Experimental autoimmune encephalomyelitis
EDTA - Ethylenediaminetetraacetic
ELISA – Enzyme-linked immune assay

F
FACS – Fluorescence-activated cell sorting
FBS – Fetal bovine serum
Foxp3 – Forkhead box p3

G
G - Gauge
GFAP – Glial fibrillary acid protein

H
HE – Hematoxylin and eosin staining

I
IFN – Interferon
Ig – Immunoglobulin
IL – Interleukin
iNOS – Inducible nitric oxide synthase

L
LCN2 – Lipocalin-2
LPS – Lipopolysaccharide

M
MBP – Myelin basic protein
MHC – Major histocompatibility complex
mL – Millilitre
MMP – Metalloproteinase
MOG – Myelin oligodendrocyte protein
MRI – Magnetic resonance imaging
MS – Multiple sclerosis

N
Neo – Neomycin
NG2 – neural/glial antigen 2
NO – Nitric oxide
NOD/Lt – Nonobese diabetic

O
OD – Optical density
OPCs – Oligodendrocyte precursor cells

P
PB – Phosphate buffer
PBS – Phosphate buffered Saline
PCR – Polymerase chain reaction
PDGFRα – Platelet-derived growth factor receptor α
PFA - Paraformaldehyde
PLP – Proteolipid protein
PP – Primary progressive
PTX – Pertussis toxin

Q

qRT-PCR – Real time quantitative polymerase chain reaction

R

RNA – Ribonucleic acid
ROS – Reactive oxygen species
RR – Relapse-remitting
RT – Room temperature
RT-PCR – Reverse-transcription polymerase chain reaction

S

SP – Secondary progressive

T

TCR – T cell receptor
TGFβ – Transforming growth factor β
Th – T helper
TIMP – Tissue inhibitors of metalloproteinases
TMEV – Theiler's murine encephalomyelitis virus
TNFα – Tumor necrosis factor α
Treg – regulatory T cells

V

VCAM – Vascular cell adhesion protein
VLA – Very late protein

W

WT – Wild-type

FIGURES LIST

Figure 1 - Proposed pathogenic pathway involved in MS.

Figure 2 - Generation of LCN2-null mice.

Figure 3 - Schematic representation of the genotype strategy for LCN2-null mice.

Figure 4 - Schematic representation of the experimental groups and the EAE induction protocol.

Figure 5 - Gating strategy used in the flow cytometry analysis.

Figure 6 - Disease course of MOG_{35-55}-induced EAE in WT animals.

Figure 7 – Thymus flow cytometry results.

Figure 8 – Corticosterone serum concentration at the sacrifice day.

Figure 9 – Histological morphology of the thymus in WT non-induced and EAE animals at the onset phase of disease.

Figure 10 – Disease course of MOG_{35-55}-induced EAE in LCN2-null mice and WT littermates.

Figure 11 – Flow cytometry results in LCN2-null and WT mice.

Figure 12 – Serum corticosterone concentration in LCN2-null and WT mice at the sacrifice day.

Figure 13 - Expression levels of inflammatory cytokines in the cerebellum.

Figure 14 – Luxol fast blue staining for myelin in cerebellum slices.

Figure 15 – GFAP immunohistochemical staining and expression levels in the cerebellum.

TABLES LIST

Table 1 – Primers' sequence for genotyping LCN2-null animals and littermates.

Table 2 – Volume of reagents and PCR reaction conditions used for the genotyping PCR reaction.

Table 3 - Mix and reaction conditions used for the RT-PCR.

Table 4 - Reaction conditions used for the qRT-PCR.

Table 5 – EAE progression in LCN2-null mice and WT littermate mice.

Table 6 - Two-Way ANOVA results for the comparison of thymus populations percentages between LCN2-null and WT mice.

Table 7 – Two-Way ANOVA results for the comparison of thymus cell numbers between LCN2-null and WT mice.

Table 8 - Results of the two-way analysis of gene expression in the cerebellum.

1. INTRODUCTION

1. INTRODUCTION

1.1 Multiple Sclerosis

Multiple sclerosis (MS) is a chronic immune mediated demyelinating disease of the central nervous system (CNS) (Lassmann & van Horssen, 2011; Noseworthy et al., 2000). In developed countries it is the second cause of neurological disability in young adults, with high burden for the patient, the family and the resources of the health system (Borreani et al., 2014). MS is a complex disease in which there is a strong immune response against the myelin sheath of CNS axons, but its underlying mechanisms are only partially understood. Most patients initially present with a clinically isolated syndrome (CIS) in early adulthood. These CIS patients present an acute episode, which typically affects one brain region, being the clinical symptoms variable depending on the involvement of motor, sensory, visual or autonomic systems. (Compston & Coles, 2008). Some CIS patients will evolve to definite MS disease, while others won't. Nowadays, the diagnosis of definite MS is based on recognized clinical criteria, with the support of magnetic resonance imaging (MRI) data and cerebrospinal fluid (CSF) analysis (Noseworthy et al., 2000), and can only be done when there is dissemination of neurologic dysfunction in space and time (Compston & Coles, 2008; Noseworthy et al., 2000; Polman et al., 2011), and after differential diagnosis have been excluded (Polman et al., 2011). Concerning the MRI findings, the presence of multifocal demyelinating lesions at different timepoints involving preferentially the periventricular white matter, the brain stem, the cerebellum and the spinal cord are indicative of MS (Noseworthy et al., 2000). Besides this, the presence of oligoclonal bands or increased concentration of immunoglobulin (Ig)G in the patients' CSF are widely used to support MS diagnosis, but are not MS-specific (Fossey et al., 2007; Noseworthy et al., 2000).

Patients with definite MS can develop different profiles of the disease. Taking in consideration the different profiles of the disease, MS can be classified as relapse-remitting (RR)-MS, primary progressive (PP)-MS or secondary progressive (SP)-MS. RR-MS represents about 80-85% of MS cases (Sospedra & Martin, 2005) and is characterized by transient symptoms (relapse) that in most of the times improve within weeks (remission). However, the ability to fully recover from relapse episodes diminishes with time, and irreversible damage accumulates in the CNS, giving rise to SP-MS. The remaining 15-20% of patients has PP-MS, and does not show this relapse-remitting pattern; rather, their symptoms become gradually worst along the course of the disease. The RR-MS presents a female to male ratio of 2:1, while in the PP-MS the incidence is similar between both genders (Noseworthy et al., 2000).

Noticeably, some CIS patients never progress to definite MS. But in those patients that do evolve, an early treatment might reduce disease severity. Taking this into account, it is crucial to find new therapeutics to reduce not only the strong pro-inflammatory reaction, but also the relapse rate and, consequently, delay irreversible damage (Comi et al., 2000). Another challenge regarding MS has been to identify the CIS patients that present a high risk of having future episodes, which would confirm the diagnosis of definite MS (Brettschneider et al., 2010). This identification could be done based on disease biomarkers, measured in the patients' blood or CSF. However, the etiology and the pathogenesis of MS are poorly understood, which makes it harder to find appropriate biomarkers for disease initiation and progression. (Lassmann & van Horssen, 2011).

1.2 Etiology of MS disease

1.2.1 Environmental and genetic factors

Regarding the etiology of MS, both environmental factors, such as infectious agents and lifestyle, and genetic factors have been proposed to induce or contribute to disease appearance (Compston & Coles, 2008; Sospedra & Martin, 2005). Among the environmental factors, the influence of viral infections is being largely addressed but until now nothing was proved. Regarding viral infections, it was shown that human herpesvirus-6 or Epstein-Barr viruses, may trigger a cascade of inflammatory events that lead to MS. In addition, because a higher proportion of women suffer from MS it was suggested that changes in hormone levels may influence disease initiation (Sospedra & Martin, 2005). Moreover, variations in sunlight exposure were also strongly associated with increased MS risk (Ebers, 2008), mostly due to changes in melatonin production. Specifically, it was shown that an excess of melatonin induced by decreased sunlight exposure enhances the Th1 response, boosting the inflammatory response (Sospedra & Martin, 2005). Finally, in the field of the genetic factors, genome-wide association studies have identified the allele for human leukocyte antigen (HLA)-DRB1*15:01 as the haplotype that represents the highest risk factor for MS (Nylander & Hafler, 2012; Sawcer et al., 2014). This haplotype explains between 14-50% of the genetic risk for MS (Hafler et al., 2005; Sawcer et al., 2014). Other susceptibility in non-HLA loci were also identified as being associated with MS, being most of them involved in the immunological response, especially in T cell immunity, like the interleukin (IL)2 receptor α gene (*Il2Rα*) and the IL7 receptor α (*Il7Rα*) gene (Berge et al., 2013; Hafler et al., 2007).

1.2.2 Onset mechanism

MS pathogenesis is fostered by a dysregulated autoimmune response. Initially, naïve myelin-specific T cells are primed in the lymph nodes by antigen presenting cells (APCs) that present myelin cross-reactive epitopes (Nakahara et al., 2010). During this process, an unknown mechanism triggers the activation of autoreactive T cells, which start to show cross-reactivity to self-antigens, such as proteins found in the myelin sheath, namely myelin basic protein (MBP), myelin oligodendrocyte protein (MOG) and proteolipid protein (PLP) (Steinman, 2001) (phase 1, Figure 1). After the initial priming of T cells, they migrate to the CNS and cross the endothelium, breaching the blood-brain barrier (BBB) (phases 2-4, Figure 1). The crossing is facilitated by the expression of the integrin very late antigen (VLA)-4 by activated T cells, which will interact with the vascular cell adhesion protein (VCAM) expressed by inflamed endothelial cells (Reboldi et al., 2009; Steinman, 2001). Likewise, activated T cells express members of the immunoglobulin superfamily, such as cluster of differentiation (CD)4 and CD8, which will interact with endothelial cells via major histocompatibility complex (MHC) class II and class I molecules, respectively. Moreover, the transendothelial migration of T cells is facilitated by metalloproteinases (MMP)2 and 9, which play a role in the degradation of the extracellular matrix, and are detectable in the CSF of MS patients (Steinman, 2001). Besides entering through the BBB, activated autoimmune T cells are also able to enter the CNS through the choroid plexus (CP), which forms the blood-CSF barrier. (Reboldi et al., 2009) Once the barriers of the brain have been breached, inflammatory cells spread into the white matter of the CNS, and are re-activated by myelin epitopes (Nakahara et al., 2010) (phase 5, Figure 1). The re-activated T cells in particular will produce cytokines and chemokines, which will promote the recruitment of other immune cells, like B cells (Miller, 2012), monocytes, and mast cells (Sospedra & Martin, 2005), from the periphery, and activate resident cells, namely microglia and astrocytes, inducing the production of nitric oxide (NO) and osteopontin (Sospedra & Martin, 2005; Steinman, 2001). Increased levels of NO are a major contributor for the death of oligodendrocytes and osteopontin induces the production of T helper (Th)1 cytokines, namely interferon (IFN)-γ and interleukin (IL)-12, and down-regulates Th2 cytokine production, contributing to an exacerbation of MS. The end result of this combined response by innate and adaptive immune cells, and respective inflammatory mediators, is the formation of an inflammatory lesion (phase 6, Figure 1), characterized by demyelinated axons, apoptotic oligodendrocytes, macrophages loaded with phagocytized myelin lipids, and activation and proliferation of astrocytes (Sospedra & Martin, 2005). It is believed that, upon lesion formation, brain cells are recruited to the injury site to promote regeneration of the tissue. In particular, oligodendrocyte precursor cells (OPCs) are recruited to the

lesion sites and differentiate into myelinating oligodendrocytes that are able to remyelinate denuded internode areas. In these areas the nerve conduction velocity is slower than before, because the myelin sheath produced is less thick than the original one, which also leads to the redistribution of sodium channels as a compensation measure (Sospedra & Martin, 2005).

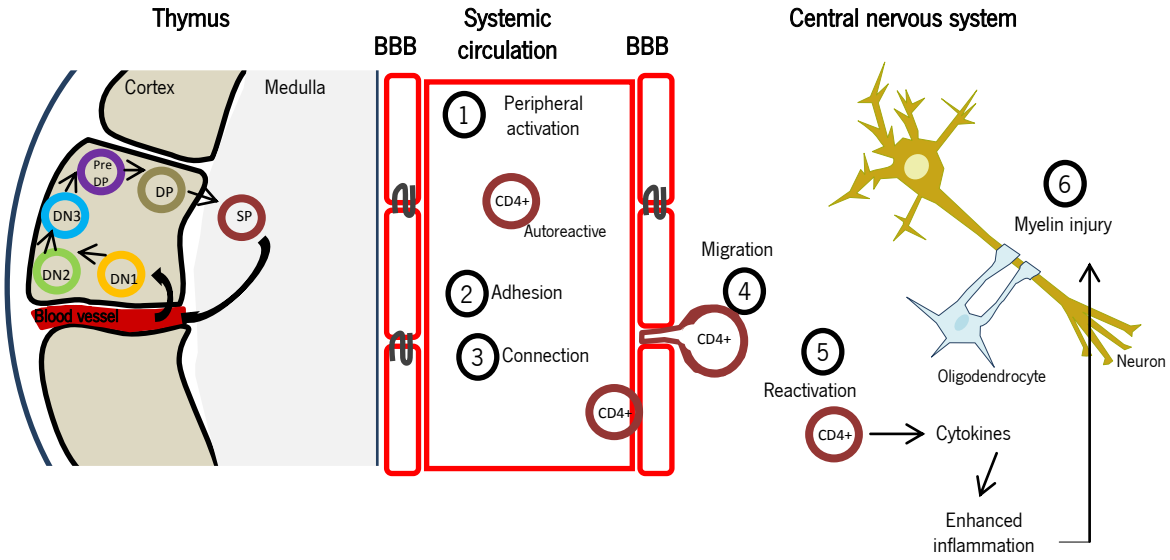

Figure 1 - *Proposed pathogenic pathway involved in MS.*

Another proposed theory for the pathogenesis of MS is the oligodendrogliopathy hypothesis. According to this hypothesis, the inflammation is not the cause of demyelination, but instead is the result of oligodendroglial apoptosis, myelin degeneration and impaired myelin regeneration. The lesions result from apoptosis of oligodendrocytes, which induce myelin degeneration and the recruitment of macrophages to eliminate the myelin debris. Consequently, immune reactions involving T and B cells occur along with a slower and poorly effective oligodendroglial regeneration and remyelination (Nakahara et al., 2010). However, considering that most of the susceptible loci identified for MS are located in genes involved in the immunological response (Berge et al., 2013), this favours the first theory, i.e. an initial immune dysregulation followed by secondary degenerative processes (Slavin et al., 2010). Nevertheless, and considering that the clinical, genetic, MRI and pathological data is heterogeneous in MS, it is highly possible that more than one pathogenetic mechanism contributes to disease establishment (Noseworthy et al., 2000), which rises the necessity for the development of therapies that not only modulate the immune response, but can also act on other disease targets, like oligodendrocytes and axons (Lucchinetti et al., 2005).

1.3 MS symptoms

MS patients usually present the first symptoms of disease between the ages of 20 and 40. Disease activity results in reversible but also in irreversible sequelae. Irreversible sequelae ultimately lead to progressive impairment and disability in the majority of patients. Common symptoms among MS patients include sensory problems, such as numbness or tingling, weakness, difficulties walking, double vision and poor coordination. However, no two patients have exactly the same symptoms. With disease progression patients start to develop increased disability, showing problems in bladder and bowel control, cognitive performance and sexual performance. They may also present fatigue, even after a good night's sleep, and walking problems. Ultimately, MS patients need wheelchair and can become bedridden (Joy & Johnston Jr., 2001).

The first symptoms presented by MS patients are widely believed to result from the exacerbated inflammatory process, which is associated with reduction of the nerve conduction velocity, and, on the other hand, the regression of symptoms correlates with the resolution of the inflammatory lesion and partial remyelination. As already mentioned, the axonal injury resultant from repeated episodes can become irreversible. In this case there is the formation of a glial scar and also there is an exhaustion of the OPCs pool, leading to progressive loss of neurological function, and to the formation of demyelinating plaques (Noseworthy et al., 2000). Altogether, the presence of focal demyelination, inflammation, glial scar formation and varying axonal damage are considered the hallmarks of MS disease (Lucchinetti et al., 2005).

Over the last years, the use of animal models has provided important insights into MS pathophysiology of MS and possible therapeutic targets. In the next section we will present the main characteristics of the animal models used to study MS, with special attention given to the experimental autoimmune encephalomyelitis (EAE) model, which is the most common animal model for studying MS.

1.4 MS animal models – Experimental autoimmune encephalomyelitis

Human studies have some limitations, such as limited access to human tissue, especially from living patients, the fact that the experimental design of clinical trials cannot be easily modified, and the fact that studies of disease mechanisms are difficult to perform in humans (Denic et al., 2011). For that reason, the importance of animal studies relies on the fact that they provide flexible, potent and rapid platforms for MS research (Ransohoff, 2012). As already mentioned, the etiology and pathogenesis of MS are still unclear, which makes it difficult to find one animal model that accurately represents all

aspects of this disease (Denic et al., 2011). Instead, there are currently three main models that are used to study different pathological characteristics of MS: (1) viral models of inflammatory demyelination; (2) demyelination induced by toxic agents; (3) inducible models of EAE (Batoulis et al., 2011; Procaccini et al., 2015). Besides these three models, there are T-cell receptors (TCR) transgenic mice models that spontaneously develop EAE (Croxford et al., 2011; Wekerle & Kurschus, 2006).

The Theiler's murine encephalomyelitis virus (TMEV) is the best characterized model of virus-induced demyelination. It is used to study how viral infections are able to induce CNS autoimmunity (Batoulis et al., 2011). In this model, the animals are inoculated with a virus, which will induce acute inflammation in the CNS, and ultimately lead to demyelination and axonal damage in the CNS (Batoulis et al., 2011; Denic et al., 2011). Susceptible mice always develop a chronic-progressive form of disease (Batoulis et al., 2011). One disadvantage of this model is the induction of a special inflammatory environment, by the virus, which is unlikely to reflect what happens in typical MS lesions (Wekerle & Linington, 2006).

Toxin-induced models of demyelination include the cuprizone and the lysolecithin models. Cuprizone is a copper chelator, which causes demyelination, with minor inflammation or axonal damage, predominantly in the cerebellar cortex and peduncle, when fed to the animals. This is a good model to study the main characteristics of focal demyelination and also remyelination (Batoulis et al., 2011; Denic et al., 2011; Fossey et al., 2007), since spontaneous remyelination is observed after withdrawal of cuprizone (Mix et al., 2010). Lysolecithin is used to induce focal demyelination, after injection directly in the white matter, which allows the control of the lesion size, nature and anatomical location (Woodruff & Franklin, 1999).

The EAE animal model has been used to study MS since the initial observation of paralysis, accompanied by perivascular infiltration and demyelination, in the pons and cerebellum of monkeys that were given repeated intramuscular injections of normal rabbit brain extracts (Rivers et al., 1933). Since then, a variety of mammals have been induced with EAE, from mice and rats, to goats and sheep (Denic et al., 2011). This is a model of antigen-specific autoimmunity against myelin, mediated by CD4+ T cells, which results in inflammatory demyelination of brain and spinal cord of induced animals (Dal Canto et al., 1995). Due to the clinical, immunopathological and histopathological similarities with MS, the EAE model is the most commonly used to study this human disease (Swanborg, 1995). This model has numerous applications, especially in the study of mechanisms involved in autoimmune-mediated inflammation, demyelination, axonal damage, immune cell migration across the BBB and regulatory mechanisms that can supress autoimmunity in the CNS (Stromnes & Goverman, 2006).

There is not one single model of EAE, but instead, the different combinations of animal species and strains, type of antigen used for immunization and the type of adjuvant employed give rise to different models, that differ from each other in the type of disease course (chronic *vs*. monophasic *vs*. relapse-remitting) (Swanborg, 1995), lesion location and involvement of B cell produced antibodies *vs*. T cell responses, sustaining the notion that antigens and immunogenetic background contribute to disease phenotype (Sospedra & Martin, 2005). As an example, Slavin and co-workers (1998) have shown that immunization of different strains of mice with the same peptide leads to different outcomes – after EAE induction with MOG_{35-55}, nonobese diabetic (NOD/Lt) mice presented a relapse-remitting course of disease, while C57BL/6 mice showed a chronic non-remitting disease, and BALB/c mice were not susceptible to disease induction (Slavin et al., 1998).

EAE can be induced actively, when the animals are immunized with CNS antigens, or passively, if autoreactive CD4+ T cells obtained from immunized animals are transferred into naïve animals (Batoulis et al., 2011; Dal Canto et al., 1995). Some of the CNS antigens used to induce EAE are purified MBP or PLP; whole spinal cord homogenates; or specific peptides, which correspond to the encephalitogenic portion of a protein for a given strain (Dal Canto et al., 1995), such as the MOG_{35-55} peptide. Unlike MBP and PLP, which together represent about 80-90% of CNS myelin proteins, MOG only accounts for 0.01-0.05% of these proteins, but its location at the outermost lamellae of the oligodendrocyte membrane makes it easily accessible to antibodies, hence its importance as a cellular and humoral target in MS and EAE (Slavin et al., 1998; Sospedra & Martin, 2005). Since the MOG_{35-55}-induced mice model, specifically in C57BL/6 mice, will be used in the context of the present thesis we will further characterize it in the next paragraph.

As previously shown, C57BL/6 mice induced with MOG_{35-55} present a chronic course of disease (Slavin et al., 1998; Sospedra & Martin, 2005), characterized by ascending paralysis resultant from the preferential attack to the spinal cord (Batoulis et al., 2011). The disease is characterized in the beginning by a limp tail, which progresses to hind and forelimbs paralysis (Stromnes & Goverman, 2006). Also multifocal and confluent areas of mononuclear inflammatory infiltrates and perivascular inflammatory cuffing in the cerebellum and hindbrain white matter are observed. The chronic disease course makes this a good model to study SP-MS (Constantinescu et al., 2011). The MOG_{35-55}-induced C57BL/6 model is particularly important in MS studies due to the increased availability of gene-modified strains on this background (Kuerten et al., 2007; Ransohoff, 2012). One disadvantage of the EAE model arises from the use of Freund's complete adjuvant (CFA) and pertussis toxin (PTX) for active disease induction. CFA contains bacterial components that are able to activate the innate immune

system, via pattern recognition receptors (Constantinescu et al., 2011), and, consequently, misrepresent the animals' general immune reactivity and confound the findings related with regulatory mechanisms (Wekerle & Kurschus, 2006). In the case of PTX, it will contribute to BBB permeabilization and facilitate autoantigen recognition in the CNS, by activating tissue-resident APCs (Kuerten & Lehmann, 2011). When it comes to all EAE models, other limitations can be pointed out, namely, the early detection of clinical signs in EAE, as compared with MS, which allows an early therapeutic intervention in the case of the animal model that cannot be translated into the human disease. Moreover, several therapies tested in EAE have proven ineffective or even harmful in human patients. These differences might be explained by the lower disruption of the BBB in MS patients, as compared with EAE-induced animals, which could prevent the therapeutic molecules from reaching their target in the CNS (Mix et al., 2010; Procaccini et al., 2015). Additionally, EAE is induced on highly inbred strains that are kept in a pathogen-free environment, with controlled temperature, light and humidity conditions, which is not representative of the various environmental and genetic factors that contribute to MS susceptibility (Handel et al., 2011). Besides, if we take into account that in the EAE model a CD4+ T cell response is induced, it becomes difficult to study the role of CD8+ T cells, which have been shown to be key players in MS pathogenesis (Procaccini et al., 2015; Ransohoff, 2012). Another difference that has been pointed out is the preferential involvement of the spinal cord in the EAE model, unlike the human disease, in which the cerebral and cerebellar cortex are more affected (Brown & Sawchenko, 2007; Procaccini et al., 2015; Ransohoff, 2012). Nevertheless, other brain structures have been proven to also be involved in the EAE model, namely the cerebellum and optic tract (Brown & Sawchenko, 2007).

Briefly, both in MS and in MS animal models there are four key pathological features: inflammation, demyelination, axonal loss or damage and gliosis (Constantinescu et al., 2011; Lucchinetti et al., 2005). So it is not surprising that glial cells also play a key role in MS pathophysiology. It was already mentioned that after T cell re-activation, in the CNS, there is the production of cytokines and chemokines which will activate microglial cells and astrocytes, leading to oligodendrocyte damage (Miller, 2012; Sospedra & Martin, 2005; Steinman, 2001). In the next section we will discuss the main characteristics of CNS glial cells and their participation in MS/EAE pathophysiology.

1.5 The role of glial cells in EAE

There are 3 types of glial cells in the mature CNS: astrocytes, oligodendrocytes and microglial cells (Purves et al., 2001), and all of them have been reported as being involved in MS pathogenesis.

1.5.1 Oligodendrocytes

Oligodendrocytes are responsible for producing myelin that wraps around some, but not all, neuronal axons. The oligodendrocyte-myelin-axon unit represent a unique structure, with specialized functions, within the CNS. Myelin contributes not only to increase the cross-sectional diameter of axons, increasing the velocity of action potential conduction, through saltatory conduction (Frohman et al., 2006; Purves et al., 2001), but also for the axonal stability, and normal neuronal functioning, by inducing sodium channel clustering, via oligodendrocyte-derived soluble factors, even in the absence of direct axon-glial contact (Chandran et al., 2008; Kuerten & Lehmann, 2011). During the course of MS and EAE, oligodendrocyte death occurs, mediated by endogenous factors, such as the activation of cell death by caspase-11 and caspase-3, via specific pathways (Hisahara et al., 2001), or by the release of cytotoxic cytokines by activated microglia and astrocytes, namely IFN-γ (Vartanian et al., 1995).

New oligodendrocytes that participate in remyelination could arise either from surviving oligodendrocytes or OPCs at the lesion sites, or from OPCs that migrate to the lesion (Reynolds et al., 2002). Taking into account that mature oligodendrocytes are post-mitotic cells, it is very unlikely that they could originate new functional oligodendrocytes. OPCs have been identified in chronic lesions, although in a relatively quiescent state (Chari & Blakemore, 2002), and have also been shown to proliferate after acute demyelination (Reynolds et al., 2002), hence they are the most probable candidates involved in remyelination. This idea is supported by studies in which, after labelling OPCs in normal white matter and inducing demyelination, it was possible to locate these cells as remyelinating oligodendrocytes. Also, the transplantation of OPCs, isolated from the adult CNS, was found to be able to remyelinate areas of demyelination (Franklin, 2002). Consequently to an acute demyelination episode, induced by chemical or immunological mechanisms, neural/glial antigen 2 (NG2)+ OPCs become reactive, proliferate, and migrate to the lesion sites (Reynolds et al., 2002). At the lesion sites, OPCs have to be able to differentiate into functional myelinating oligodendrocytes (Chari & Blakemore, 2002).

Different theories try to explain why remyelination fails in MS. One of the most popular theories claims that failure in remyelination arises from exhaustion of the pool of OPCs, induced by repeated episodes of inflammation and demyelination (Reynolds et al., 2002). It could also be that the local OPCs present

are not able to further differentiate into myelinating oligodendrocytes, due to the lack of differentiation signals or to the presence of inhibitory signals (Back et al., 2005; Franklin, 2002), such as hyaluronan (Williams et al., 2007).

In addition, studies using organotypic cultures of cerebellum, challenged with lipopolysaccharide (LPS), have shown microglia activation, characterized by morphological changes from ramified to amoeboid shaped cells, the production of pro-inflammatory cytokines, like IL-1β, IL-6 and tumor necrosis factor (TNF)-α, and the induction of oxidative stress, via production of reactive oxygen species (ROS) and inducible nitric oxide synthase (iNOS) (di Penta et al., 2013). This microglia activation was associated with oligodendrocyte death, and myelin and axonal damage (di Penta et al., 2013).

1.5.2 Microglia

Microglial cells are considered to be the macrophages of the brain, due to their myeloid origin, ability to circulate and migrate within different regions of the brain, and to phagocyte, process and present antigens. In this sense, microglial cells are the CNS-resident immune cells, functioning as the first line of defense against immune and inflammatory stimuli (Lee et al., 2007). Under physiological conditions, resting microglia play a crucial role in the immune surveillance of the brain, interacting with the other brain cells and actively monitoring and remodelling impaired synapses. Subsequently to CNS damage, the number of microglial cells increases dramatically at the lesioned site, due to proliferation of resident microglia and migration of monocytes, from circulation (Purves et al., 2001). These cells share many properties with tissue macrophages, namely they are scavenger cells that remove cellular debris from injury sites (Purves et al., 2001). This phagocytic removal of apoptotic cellular material, without induction of inflammation, is one of the main beneficial roles of microglia. However, microglial cells are unable to efficiently remove myelin debris when Wallerian degeneration is associated with acute injury, preventing axonal regeneration. Principally after activation, these cells are able to secrete important pro- or anti-inflammatory mediators that act as paracrine mediators of neural cell migration and survival, but may also promote the autocrine polarization of microglia into different states of activation, the M1 and M2 microglia. In the first case microglial activation is more harmful, and in the second is more protective. Furthermore, microglial cells are involved in CNS repair, by producing cytokines and chemokines, but can also induce oligodendrocyte death through the production of cytotoxic molecules. Another beneficial function that has been attributed to microglia is the ability to recruit stem cells and induce neurogenesis (Napoli & Neumann, 2010). In response to an inflammatory stimuli, microglia upregulate CD45, CD86, CD80, CD40 and MHC-class II, enhancing their ability to function as APC

(Minagar et al., 2002; Murphy et al., 2010). Moreover, persistent activation of microglia contributes to increase the permeability of the BBB, and promotes the infiltration of peripheral macrophages (Miller, 2012). It was already referred that MMP2 and MMP9 are important in MS pathogenesis, more specifically, for facilitating T cell transendothelial migration (Steinman, 2001). In the CNS, these two MMPs are secreted by microglia and astrocytes as active forms (Nakanishi, 2003). Thus, microglia can exert both beneficial and detrimental functions during disease development, depending on the stage and context of a given lesion (Correale, 2014).

1.5.3 Astrocytes

Astrocytic involvement in MS has long been recognized. A few years before Charcot described a disease, which he called "Sclérose en plaques", in 1868, Rindfleisch had already described the presence of multinucleated cells with processes in a CNS pathology named "grey degeneration". These cells were later identified as astrocytes (Williams et al., 2007). In physiological conditions, astrocytes play an essential role in maintaining survival of neurons and other glial cells (Miller, 2012), by providing structural support to neurons (Nair et al., 2008), maintaining the extracellular ionic environment and pH and secreting metabolic substrates for neurons (Sofroniew, 2005). They are also able to actively alter the synaptic transmission by clearing and releasing extracellular glutamate from/to the synaptic cleft (Nair et al., 2008; Sofroniew, 2005). In addition, perivascular astrocytes are tightly associated with the basal lamina of blood vessels, contributing for the maintenance of the BBB (Brambilla et al., 2014). Following a CNS insult, like injury, ischemia and neurodegeneration, astrocytes become reactive and suffer morphological changes, such as cytoplasm enlargement, increased size and ramification of processes (Lee et al., 2009), upregulation of glial fibrillary acidic protein (GFAP) and vimentin, and re-expression of nestin (Williams et al., 2007). Astrocytes, along with microglial cells, play a dual role in protection and injury in MS (Minagar et al., 2002).

In situations of CNS insult, astrocytes upregulate the expression of glutamate transporters and glutamine synthetase, preventing the extracellular accumulation of glutamate, and consequently its excitotoxic effects on neurons and oligodendrocytes (Nair et al., 2008; Sofroniew, 2005). Also, astrocytes produce chemokines, that are able to recruit OPCs to demyelination sites (Williams et al., 2007), and anti-inflammatory cytokines, such as IL-10, IL-4, IL-5, IL-27 and transforming growth factor (TGF)-β (Nair et al., 2008). The formation of a reactive scar by astrocytes, on one hand, helps to surround and separate the damaged tissue from normal white matter, but on the other hand, presents as a major obstacle for axon regeneration (Sofroniew, 2005). The gliotic scar could also result from a

failed attempt of remyelination (Franklin, 2002). In addition, astrocytes further contribute for the permeabilization of the BBB by secreting IL-6, TNF-α and IL-1β, which will act specifically on endothelial cells and tight junctions (Nair et al., 2008). As mentioned previously, astrocytes can express MMPs (Nakanishi, 2003), but they are also able to express tissue inhibitors of metallopeptidases (TIMP)-1, that regulate negatively the activity of MMPs (Nair et al., 2008; Williams et al., 2007).

Reactive GFAP+ astrocytes were found in the spinal cords of Lewis rats induced with EAE, even before the appearance of disease clinical symptoms (Smith et al., 1983). Also, in a mice model of EAE with a chronic relapsing disease course [model characterized by both relapsing-remitting episodes, with inflammatory-mediated demyelination, and progressive disease, with axonal and neuronal loss (Ramaglia et al., 2015)], astrocytic activation was found at lesion sites, and *Gfap* expression levels were found to fluctuate according to the symptomatic stage of disease (Kothavale et al., 1995). Of relevance, when a drug that targets glial activation was used, it seems that there was a reduction in both clinical and pathological severities of EAE, namely there was a partial rescue of oligodendrocytes from cell death (Guo et al., 2007). Previously, GFAP-null mice induced with EAE presented a more severe clinical course, supporting the importance of GFAP in structural stabilization of the white matter (Liedtke et al., 1998). Altogether, these findings suggest that an excessive glial response is deleterious for EAE recovery, but a defective glial response is also unable to delimitate lesion sites, and protect the healthy surrounding tissue from secondary degeneration.

Previous *in vitro* and *in vivo* studies from our laboratory have shown the production by astrocytes of an acute-phase protein, lipocalin-2 (LCN2), in response to different inflammatory stimuli, namely in the EAE context. We will further assess this subject and describe the possible involvement of LCN2 in MS and EAE pathogenesis.

1.6 Lipocalin-2

Lipocalin-2 (LCN2), also known as neutrophil gelatinase-associated lipocalin (NGAL) or 24p3, was first identified by Kjeldsen and colleagues (1993) as a protein present in neutrophil granules, partly covalently associated with human neutrophil gelatinase (Kjeldsen et al., 1993, 1994). LCN2 is a member of the lipocalin family, whose members are characterized by a compact tertiary structure, with a central hydrophobic core that allows the binding to small lipophilic substances (e.g. retinol), along with an ability to bind specific cell-surface receptors and to covalently associate with other proteins, leading to the formation of molecular complexes (Flower, 1996; Kjeldsen et al., 1994).

Initial reports described LCN2 as an acute phase protein in mice, involved in acute responses to various inflammatory or stressful stimuli (Q. Liu & Nilsen-Hamilton, 1995; Marques et al., 2008).

The particular production of LCN2 upon bacterial infection is suggested to occur as part of the innate immune response (Flo et al., 2004). Invading pathogens, when confronted with the low levels of iron present in the host, and in order to proliferate, secrete siderophores, small binding molecules that have higher-affinity to iron than the endogenous host iron-trafficking proteins. To cope with this, and at the site of infection, neutrophils release LCN2, which will then bind specifically to the bacterial ferric siderophores, preventing iron from being transported into the bacteria (Flo et al., 2004; Goetz et al., 2002). The importance of this mechanism is demonstrated by the fact that LCN2-null mice have increased susceptibility to bacterial infection (Flo et al., 2004).

More recently, LCN2 was also found to interact with endogenous iron (Yang et al., 2002) using an endogenous mammalian siderophore [2,5-dihydroxybenzoic acid (2,5-DHBA)] (Bao et al., 2010; Devireddy et al., 2010) and to be able to deliver this iron to cells in culture, independently of transferrin delivery system (Yang et al., 2002). In fact, a model of iron trafficking by LCN2 was proposed, where LCN2 lacking iron (apo-LCN2) binds to 24p3 receptor (24p3r), is internalized and binds to an intracellular mammalian siderophore, chelates iron and is exocytosed from the cell, decreasing intracellular iron concentration. On the contrary, holo-LCN2 binds to 24p3r, is internalized, traffics to endosomes and releases iron from the complex, thereby increasing intracellular iron concentration. Importantly, this LCN2-mediated modulation of cell iron content has been shown to impact on cell proliferation and apoptosis , since apo-LCN2 internalization results in apoptosis and cell death through the pro-apoptotic B cell lymphoma 2 (Bcl-2)-interacting mediator of cell death (BIM) protein (Devireddy et al., 2005).

1.6.1 Lipocalin-2 and CNS

In what concerns LCN2 and CNS, current literature is not consensual in defining the real function of LCN2, neither by which cells it is produced. In response to a peripheral immune challenge, such as the intraperitoneal injection of LPS, *Lcn2* expression is quickly upregulated in the CP, which is a thin membrane present in the brain ventricles that produces the majority of the CSF. As a result of this upregulation, LCN2 protein levels in the CSF are also increased. Immunohistochemical stainings in the CP have shown positive labelling for LCN2 in some, but not all, epithelial cells, suggesting that only certain cells express detectable amounts of LCN2, at least at a given moment. In this study, also the endothelial cells seemed to be able to produce LCN2 (Marques et al., 2008). In addition, using the

same LPS-injection model, another group confirmed the LCN2 production by CP-associated cells and by endothelial cells, but they also showed that microglial cells were able to produce it, which is controversial in the literature (Ip et al., 2011). The production by astrocytes is more accepted, in several inflammatory conditions, and even in physiological conditions (Chia et al., 2011). Cultured astrocytes stimulated with LPS, TNF-α and amyloid-β_{1-42} are able to upregulate LCN2 expression and secretion (Lee et al., 2009; Mesquita et al., 2014). Regarding the role of LCN2 in astrocytes, it seems that LCN2 is able to polarize astrocytes into a more inflammatory phenotype (Jang et al., 2013). In accordance, *in vitro* studies, using astrocyte cultures, have reported increased sensitivity of these cells for NO-induced apoptotic death, as well as H_2O_2- and paraquat-induced necrotic cell death, mediated by LCN2.

In addition, the absence of LCN2 has been reported to affect emotional and cognitive behaviour. Specifically, when compared to wild-type (WT) animals, 10-weeks old male LCN2-null mice presented anxiety and depressive-like behaviours, which were associated with increased levels of corticosterone production, along with mild spatial reference memory impairments. This behavioural phenotype was correlated with overall alterations in hippocampal neuronal morphology, suggesting a role for LCN2 in neuronal plasticity and behaviour (Ferreira et al., 2013).

1.6.2 Lipocalin-2 and MS

As for CNS diseases, LCN2 has been implicated in the pathophysiology of Alzheimer's disease (Choi et al., 2011; Naude et al., 2012), pain (Jha et al., 2014) and MS (Berard et al., 2012; Marques et al., 2012; Nam et al., 2014). Moreover, in a relapse-remitting EAE mice model, the analysis of transcriptome of the CP showed that *Lcn2* was one of the most significantly up-regulated genes during the onset and relapse phases of disease, with a reduced expression during the remission phase. These results were correlated with high LCN2 CSF levels during the active phases of the disease, and low levels in the remission phase. Interestingly, aside from CP infiltrating neutrophils, astrocytes were found to be the only cells expressing LCN2. The production of LCN2 by the astrocytes was restricted to the brain areas that are typically affected in MS patients (Marques et al., 2012). Of relevance, LCN2 levels were also found to be elevated in CSF (Marques et al., 2012) and serum samples (Berard et al., 2012) from MS patients, when compared with healthy controls.

Specifically for MOG_{35-55} induced EAE in LCN2-null mice, the published results are contradictory. Berard and colleagues (2012) have shown that LCN2-null mice induced with EAE present a more severe disease and pro-inflammatory response, when compared to WT induced animals (Berard et al., 2012), while Nam and co-workers (2014) reported that induced LCN2-null mice presented a significant

decrease in disease severity accompanied by reduced inflammatory infiltration, glial activation, inflammatory cytokine/chemokine expression, demyelination in the spinal cord and autoreactive T cell proliferation (Nam et al., 2014).

Nevertheless, taking into account all the known functions of LCN2, there is no doubt that it plays a role in CNS inflammation, specifically in autoimmune diseases like MS. For that reason, in our study we intend to further understand and clarify if LCN2 plays a detrimental or protective role in MOG_{35-55}-induced EAE. Contrary to the mentioned published data, we will give special attention to the cerebellum, which is a brain region known to be affected in MS, and to the thymus, not often looked at, but no less important if we consider that it is the organ were T cells mature. In the next section we will make a description of the thymus, and present the data that is known regarding its involvement in MS and EAE development.

1.7 Role of the thymus in MS and EAE development

The thymus is a primary lymphoid organ, where bone marrow derived progenitor cells undergo differentiation and maturation, to originate a functional T cell repertoire (Pearse, 2006). This organ is surrounded by a thin layer of connective tissue, which gives rise to septae, in some species, that partially subdivide the thymus into lobules that interconnect with each other. In mice there is no distinct sublobulation. The cortex is constituted by packed, small, immature lymphocytes, few epithelial cells and phagocytic macrophages (Pearse, 2006). These macrophages phagocyte the lymphocytes that present high avidity for self-antigens, and that are negatively selected to die (Takahama, 2006). The medulla presents less cellular density, staining paler that the cortex, and contains more mature T cells, which are larger and have more cytoplasm than cortical T cells (Pearse, 2006). Between the cortex and the medulla, it is possible to recognize a cortico-medullary region, rich in blood vessels, thought which the prothymocytes enter the thymus (Schuurman et al., 1997).

During fetal development, hematopoietic stem cells migrate from the yolk sac and/or fetal liver to the thymus to begin thymic differentiation. In the adult thymus the differentiation process is also recapitulated by bone-marrow-derived stem cells that continually migrate to the thymus. However, in this last case there is a dynamic equilibrium between the stem cells that enter the thymus, and the mature cells that leave it. Early differentiation processes occur in the cortex of the thymus, and later ones in the medulla (Zuniga-Pflucker & Lenardo, 1996).

One of the first events taking place during thymocyte differentiation is the induction of CD25 expression in CD117+/CD44+/CD4-/CD8- thymocytes (pro-T cell stage). Thymocytes lose the expression of both CD44 and CD117, and increase the expression of CD25 (early pre-T cell stage). During this phase the first checkpoint of thymocyte differentiation occurs: the β selection, during which there is the *Tcrb* gene rearrangement, and the cells begin to assemble TCR-β and pre-TCRα chains to form the pre-TCR complex (Zuniga-Pflucker & Lenardo, 1996). If TCR gene rearrangement has been successful, thymocytes differentiate to double positive (DP) cells, which lose expression of CD25 and gain expression of either CD4 or CD8; if not, thymocytes die by apoptosis (late pre-T cell phase) (Michie & Zuniga-Pflucker, 2002; Takahama, 2006). Still in the cortical layer of the thymus, there is TCR engagement with MHC class I or class II molecules, resulting in positive selection (Goldrath & Bevan, 1999). The positive selection process ensures that thymocytes have a minimal reactivity for self-peptides, allowing only the further maturation of cells restricted to self-MHC. On the other hand, thymocytes that present high-avidity interactions to self-peptides are negatively selected and are further eliminated by apoptosis (Savage & Davis, 2001). This process of negative selection is very important for preventing autoimmunity, since it allows the elimination of the self-reactive T cells. There are also DP thymocytes that fail to receive TCR signals and are also destined to die at this stage (Takahama, 2006). The low-affinity recognition of self-MHC during the positive selection is also responsible for determining commitment to either the CD4 or CD8 lineage. Recognition of MHC class I results in CD8+ T cells, while the recognition of MHC class II results in CD4+ T cells (Goldrath & Bevan, 1999). Thymocytes that have been positively selected, and have committed to a CD4 or CD8 lineage, go to the medullary layer and interact with thymic epithelial cells to complete thymocyte maturation (Takahama, 2006). At the medulla, self-reactive thymocytes that have escaped negative selection in the cortex are further deleted. This additional deletion is particularly important in establishing central tolerance to tissue-specific antigens. The survival single positive cells are then exported from the thymus into circulation (Takahama, 2006).

Even after two negative selection checkpoints, at the cortex and the medulla of the thymus, some auto-reactive T cells are able to escape to the periphery. For example, encephalitogenic peptides, like the MBP NAc1-11 peptide, were found to bind weakly to MHC, forming unstable peptide/MHC complexes. In this case the negative selection of the T cells specific for this peptide is not efficiently mediated, allowing some of them to escape to the periphery (Song et al., 2006). Nevertheless, in the periphery the activity of auto-reactive T cells is controlled by regulatory T (Treg) cells, avoiding autoimmune diseases. Treg cells recognize mainly self-antigens, but they don't proliferate after encountering these

antigens – they are in an anergic state. Instead, when activated, Treg cells inhibit the proliferation of effector T cells in their surroundings (Rose, 1994). Hence, the thymus plays an important role in the control of organ-specific autoimmunity by limiting the development of autoreactive T cells, for which the tolerance to self-antigens is essential, and also by generating Treg cells. Of notice, an inverse correlation between MBP expression in the thymus and EAE susceptibility was found (H. Liu et al., 2001).

The role of thymus in EAE has previously been addressed by different authors with thymectomized animals. The EAE induction in animals thymectomized soon after birth or at a young age showed a significant delay in disease onset. In contrary, animals thymectomized 10 days after EAE induction did not present differences in the course or characteristics of disease when compared with sham thymectomized animals (Flechter et al., 1984). In another study, after thymectomy or sham surgery performed at 6 weeks of age, both groups of animals developed a similar disease course. However, after day 16 post-disease induction, the animals subjected to sham surgery presented an improvement in their clinical score, unlike thymectomized animals. This recovery was probably due to accelerated differentiation and proliferation of thymic CD4+ forkhead box p3 (Foxp3)+ Treg cells. In thymectomized animals, the recovery from EAE was severely impaired due to the absence of new Treg cell emigrants, which suggested that the pre-existing peripheral Treg pool alone was not sufficient for complete regulation of pathogenic T cells (Chen et al., 2009). So it seems that the thymus plays a pivotal role in EAE development, and that the age at the time of thymectomy influences the resistance or susceptibility for EAE establishment.

Although, it is widely recognized the vital role of the thymus in MS/EAE pathogenesis, it is still lacking a characterization of this organ in the WT C57BL/6 mice induced with EAE, namely regarding thymocyte populations and thymus histological morphology during disease onset and development, which we will also address in this thesis. In addition, the impact of LCN2 on this process will be evaluated.

1.8 Research objectives

Although, the initial and principal aim of the present thesis is to assess whether and how LCN2 modulates the severity of MS, because there is still limited amount of information regarding the alterations that occur in the thymus during disease development, even in WT mice, our first objective is to:

1. Characterize the main thymic populations and the histological morphology of the thymus, in WT C57BL/6 mice induced with EAE, at the onset and chronic phases disease.

To address the need to better understand the role of LCN2 in the pathophysiology of MS we will take advantage of the EAE model and of the mouse targeted deletion of *Lcn2*, and considering that most EAE studies are focused on the spinal cord, and few have studied the cerebellum, an area known to be affected in MS disease, we proposed to:

2. Study, in the cerebellum, the expression of inflammatory cytokines, evaluate the presence of inflammatory infiltrates and explore astrocytic activation, at the onset and chronic phases of disease, after inducing EAE in LCN2-null mice and WT littermates. Also, we will address the thymus to unravel the impact of LCN2 in the T cell differentiation and maturation.

2. EXPERIMENTAL PROCEDURES

2. EXPERIMENTAL PROCEDURES

2.1 Mice

All experiments were conducted in accordance with the Portuguese national authority for animal experimentation, *Direcção Geral de Veterinária* (ID: DGV94457). Animals were housed and handled in accordance with the guidelines for the care and handling of laboratory animals in the Directive 2010/63/EU of the European Parliament and of the Council. Efforts were made to minimize the number of animals used and their suffering.

The animals were housed and maintained in a controlled environment at 22-24°C and 55% humidity, on 12 hours light/dark cycles (lights on at 8 a.m.) and fed with regular rodent's chow and tap water *ad libitum*.

Experiments were performed using mice with a target deletion of the *Lcn-2* gene (LCN2-null animals) and their respective littermate controls, the WT animals. These mice were obtained from LCN2 heterozygous mattings, which in turn were obtained by breeding WT animals with LCN2-null mice in which the coding sequence (exons 2 to 5) of the gene that encodes for LCN2 was replaced by a neomycin cassette (Figure 2) (Flo et al., 2004). All the animals used were raised in a C57BL/6J background.

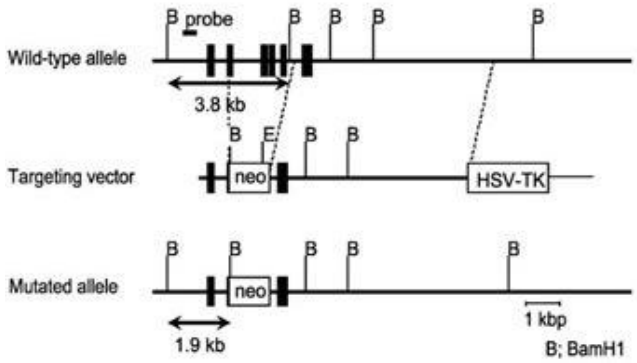

Figure 2 - *Generation of LCN2-null mice*. The entire coding sequence of the LCN2 gene was replaced by a neomycin cassette. (Adapted from Flo et al., 2004).

2.1.1 Genotyping

For the LCN2-null mice and respective WT littermates, animals' selection occurred after confirming their genotype by polymerase chain reaction (PCR). After collecting a tissue sample from the animals (ear, tail or toe sample), DNA was extracted using a DNA extraction kit (F-140; Life Technologies, Thermo

Fisher Scientific, Waltham, MA, USA). Briefly, the samples were incubated with 10µL of Dilution Buffer and 0.5µL of DNARelease Additive for 5 minutes at room temperature (RT). The tubes were then placed into the pre-heated block at 98°C for 2 minutes, centrifuged and the supernatant containing the DNA quantified using the NanoDrop 1000 spectrophotometer (Thermo Fisher Scientific).

The genotype PCR reaction and the detection of both mutated and WT alleles was performed using a common primer, which in combination with either the WT primer or the *neo*1500 primer allows to distinguish the WT from the LCN2-null mice, respectively (Figure 3).

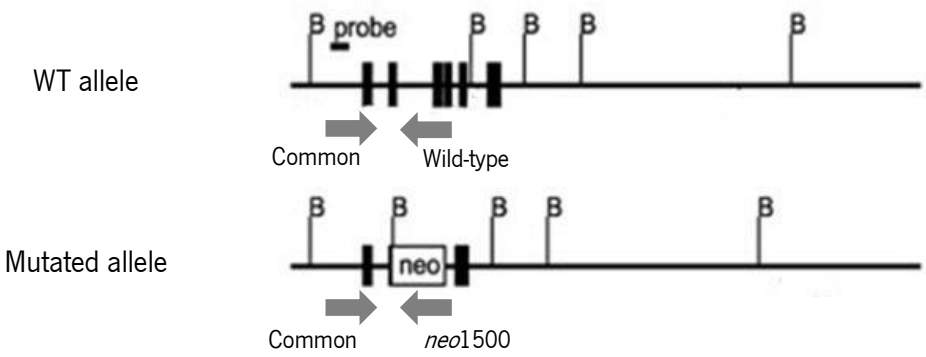

Figure 3 - *Schematic representation of the genotype strategy for LCN2-null mice.* The combination of Common and WT primers or Common and neo1500 were used to amplify the WT and the mutated alleles, respectively. (Adapted from Flo et al., 2004).

The sequences of the 3 primers used are presented in Table 1.

Table 1 – Primers' sequence for genotyping LCN2-null animals and littermates.

Primer abbreviation	Primer sequence	MT (°C)
Common	5' – CAC ATC TCA TGC TGC TCA GAT AGC CAC – 3'	58
Wild-type	5' – GTC CTT CTC ACT TTG ACA GAA GTC AGG – 3'	
*Neo*1500	5' – ATC GCC TTC TAT CGC CTT CTT GAC GAG – 3'	

MT, melting temperature.

Considering that the amplification products for both the WT and the mutated alleles have equal molecular weights (500bp), two independent PCR reactions were done for each sample. For each PCR reaction, 1µL of DNA (approximately at 100ng/µL) was added to 19µL of PCR mix, using the reagents described in Table 2. The reaction took place in a Primus 96 Plus Thermal Cycler (MWG Biotech, Ebersberg, Germany) using the conditions also presented in Table 2.

Table 2 – Volume of reagents and PCR reaction conditions used for the genotyping PCR reaction.

Master mix (vol. 20µL)	Volume/µL	DNA template	PCR conditions
H_2O (Milli Q) [1]	14.5	1 µL (100ng/µL)	95°C 2'
Taq buffer (with $(NH_4)_2SO_4$) [2]	2		95°C 1'
$MgCl_2$ (25mM)	1.2		58°C 45''
dNTPs (10mM)	0.4		72°C 1' (30 cycles)
Primer 1 (10µM) [3]	0.4		72°C 5'
Primer 2 (10µM) [4]	0.4		4°C ∞
Taq polymerase (5U/µL)[2]	0.1		

[1] 95284, Sigma-Aldrich®; [2] Fermentas Life Science, CA, USA; [3] Primer Common; [4] Primer Wild-type or *Neo*1500

The PCR amplification products were electrophoresed on a 1% agarose gel, after staining with GreenSafe Premium (MB13201; NZYTech, Lda., Genes and Enzymes, Lisboa, Portugal), and detected under UV light using a Gel Doc™ EZ Imager (Bio-Rad Laboratories, Hercules, CA, USA). The WT and the LCN2-null mice were identified for presenting only one band, for one of the PCR reactions, while the heterozygous animals presented 2 bands.

2.1.2 EAE induction

Experimental autoimmune encephalomyelitis (EAE) was induced in the animals with the Hooke Kit™ MOG_{35-55}/CFA Emulsion PTX (EK-2110; Hooke Laboratories, Lawrence, MA, USA). For that, LCN2-null females and respective WT littermates, at 10-16 weeks of age were subcutaneously injected with an emulsion of MOG_{35-55} in Freund's complete adjuvant (CFA), at the upper and lower back of the animal, followed by an intraperitoneal administration of pertussis toxin (PTX) in PBS, at a final concentration of 217ng/mL, after 2 and 24 hours of immunization. Non-induced animals, both WT and LCN2-null mice, were injected subcutaneously with an emulsion of PBS in CFA (263810; Difco Laboratories, Detroit, USA), and were also injected with PTX at the same time as the EAE animals (Figure 4).

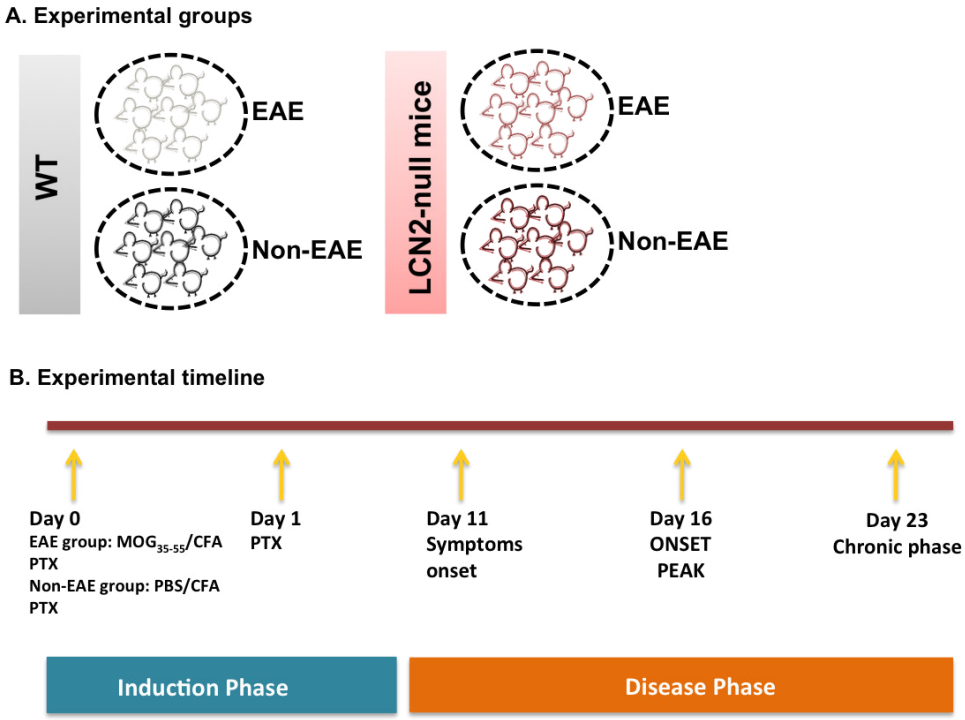

Figure 4 - *Schematic representation of the experimental groups and the EAE induction protocol.*

All animals were daily weighted and monitored for clinical symptoms of disease, in a blinded way. Disease severity was scored according to the scale previously described by Stromnes and Goverman (Stromnes & Goverman, 2006), with few changes, as follows: 0=no clinical signs; 0.5=partially limp tail; 1=paralyzed tail; 1.5=at least one of the hind legs falls through consistently when the animal is dropped on a wire rack; 2=loss in coordinated movement, wobbly walk; 2.5=dragging of the hind limbs;3=paralysis of both hind limbs; 3.5=hind limbs paralyzed and weakness in forelimbs; 4=complete hind limbs paralysis and partial forelimbs paralysis; 4.5=animal is not alert, no movement; 5=moribund state or found dead.

2.1.3 Sample collection

For biological sample collection, a group of EAE animals, both WT and LCN2-null mice, were sacrificed at the onset phase of disease (16 days after EAE induction), and another at the chronic phase of disease (21 or 23 days after EAE induction). Non-induced animals, from both genotypes, were sacrificed following the same experimental timepoints. Animals were anesthetized with ketamine hydrochloride (150mg/Kg) plus medetomidine (0.3mg/Kg). Blood was collected from the inferior vena

cava for posterior analysis, and animals were transcardially perfused with cold saline. Tissues collected included the brain, the thymus and the spinal cord.

Brains collected were either macrodissected, for further gene expression studies, or immediately embedded in Tissue-Tek® O.C.T.™ compound (4583; Sakura Finetek, Japan), frozen on liquid nitrogen and kept frozen at -20°C until further processing for immunohistochemistry analysis. In the macrodissected brains, regions such as the cerebellum, hippocampus and hypothalamus were collected.

Similarly, the animals' thymi were collected and snap-frozen on dry ice, for gene expression studies, or harvested and dissociated for flow cytometry. Also thymus from WT animals, induced or not with EAE, were collected to evaluate histological alterations. Half of the tissue was fixated in PFA 4% and impregnated in paraffin, and the other half was embedded in Tissue-Tek® O.C.T.™ compound and frozen in liquid nitrogen, and kept at -20°C until posterior processing.

2.2 Flow cytometry

For flow cytometric analysis, the thymus of the animals was mechanically disrupted in a 6 well-plate, using 3mL of DMEM with 10% FBS. The medium was then transferred to a 15mL falcon and, after sedimentation, the supernatant, which contained the cells, was transferred to a new falcon. The tubes were then centrifuged and the pellet was resuspended in 2mL of FACS buffer. To count the total number of cells, the suspension was diluted 1:100 in a 96 well-plate, in FACS buffer, and 7-ADD was added. After 10 minutes of incubation, cells were counted in the MUSE® cell analyser (Merck Millipore, Darmstadt, Germany).

The flow cytometry analysis was performed using $1x10^6$ cells, that were incubated with a mix of the following primary antibodies: Brilliant Violet 421-anti-CD3 (clone 145-2C11, 1:100; BioLegend, San Diego, CA, USA), PercpCy5.5-anti-CD4 (clone RM 4-5, 1:400; BioLegend) and V500-anti-CD8 (clone 53-6.7, 1:50; BD Biosciences, Franklin Lakes, NJ, USA). After the incubation, samples were washed twice with FACS buffer (0.5% BSA in PBS buffer, 0.01% Azide) and resuspended in 200µL of FACS buffer. All samples were acquired on a BD LSR II flow cytometer using FACS DIVA software (BD Biosciences).

Three independent sets of animals were used, with a total of 43 WT and 41 LCN2-null mice. Data were analysed using FlowJo software (Tree Star, Ashland, OR, USA). The gating strategy (Figure 5) was as follows: single cells were gated using the FSC-H *vs.* FSC-A plot; cell debris were excluded using the SSC-

A *vs.* FSC-A plot; the CD4 and CD8 single positive, DP and DN populations were gated in the CD8 *vs.* CD4 plot within total cells; the expression of CD3 was evaluated within the single positive populations.

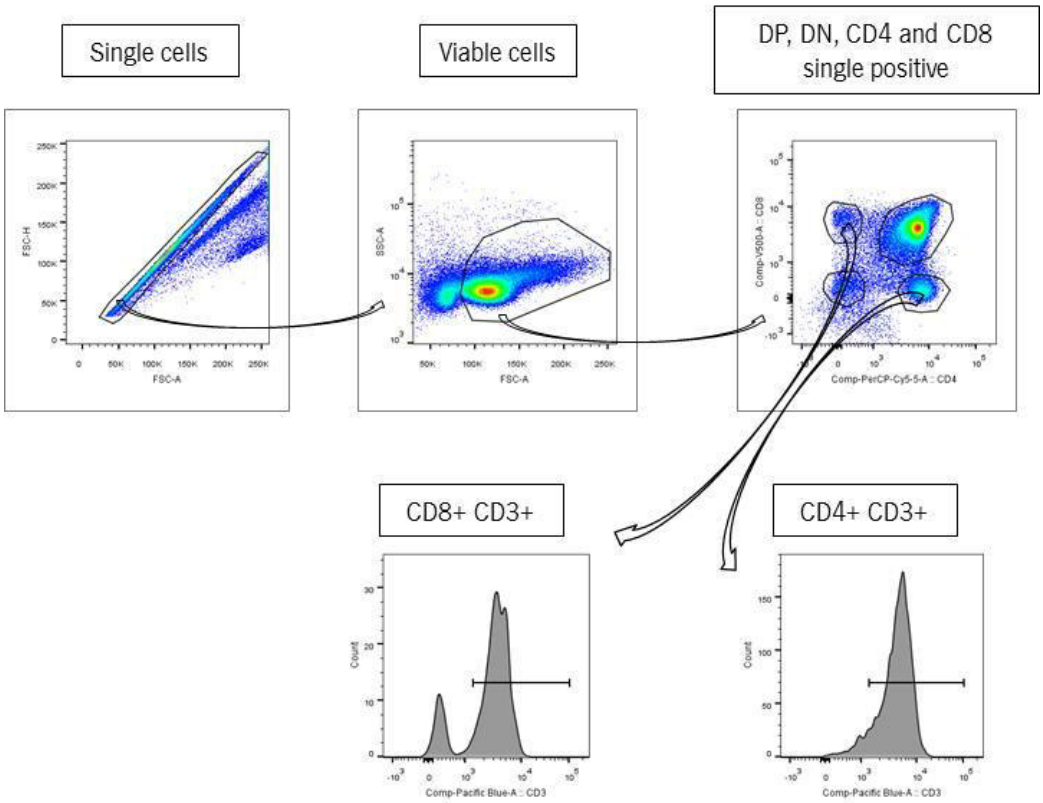

Figure 5 - *Gating strategy used in the flow cytometry analysis.*

2.3 Gene expression analysis

The expression levels of genes of interest were evaluated using real-time quantitative PCR (qRT-PCR). Total RNA was extracted from the cerebellum using TRIzol® reagent (15596; Life Technologies), according to the manufacturer's instructions. Briefly, 1mL of TRIzol® was added to the frozen tissue, which was mechanically disrupted using a 20G needle, after which 200µL of chloroform were added. The two solutions were mixed and samples were incubated 2-3 minutes at RT. After centrifugation, 3 phases were visible: an upper aqueous phase, which contains the RNA, a lower red phenol-chloroform phase and an interphase, which contain DNA and proteins. The upper phase was transferred into a new eppendorf tube, and 500µL of isopropanol were added to precipitate the RNA. Samples were incubated 10 minutes at RT. After centrifugation, the RNA pellet was washed with 75% ethanol and dissolved in 10 µL of nuclease free water (W4502; Sigma-Aldrich®). RNA quantification was performed using the NanoDrop spectrophotometer and diluted to a final concentration of approximately 1µg/µL.

Before the synthesis of cDNA, 4µL of RNA were treated with DNase, to eliminate possible DNA contamination. Briefly, the RNA was added to a RNase free tube, together with 10x reaction buffer with $MgCl_2$ (B43; Life Technologies), DNase I 1U/µg (EN0525; Life Technologies) and nuclease free water, and incubated at 37°C for 30 minutes. After adding 0.5M EDTA (R1021; Life Technologies) the tubes were placed in the pre-heated block at 65°C for 10 minutes. The tubes were then transferred to ice and the RNA was quantified again.

500ng of RNA from each sample were reverse transcribed into cDNA using the commercial kit iScript™ cDNA synthesis kit (170-8890; BioRad Laboratories, Hercules, CA, USA). Briefly, the RNA was added to a PCR tube, plus iScript reaction mix, iScript reverse transcriptase and nuclease free-water (Table 4). The reverse transcription reaction occurred in a Primus 96 Plus Thermal Cycler (MWG Biotech), accordingly to the conditions presented in Table 3.

Table 3 - Mix and reaction conditions used for the RT-PCR.

RT-PCR reagent	Volume (µL)/reaction	RT-PCR conditions
RNA	Corresponding to 500ng of RNA	5 minutes at 25°C
5x iScript reaction mix	4	30 minutes at 42°C
iScript reverse transcriptase	1	5 minutes at 85°C
Nuclease-free water	Until a final volume of 20µL	∞ at 4°C

qRT-PCR was performed on a CFX96™ Real-Time System instrument (Bio-Rad Laboratories), with the commercial kit SsoFast™ EvaGreen® Supermix (172-52; BioRad Laboratories), according to the manufacturer's instructions (Table 4), using equal amounts of cDNA from each sample. Briefly, for each sample a mix was prepared with 3µL of nuclease-free water, 5µL of SsoFast™ EvaGreen® Supermix and 0.5µL of each primer. Product fluorescence was detected at the end of the elongation cycle. All melting curves exhibited a single sharp peak at the expected temperature. The reference gene hypoxanthine guanine phophoribosyltransferase (*Hprt*) was used as an internal standard for the normalization of the expression of selected transcripts. The sequences and respective annealing temperatures of the selected transcripts are presented in Annex 1.

Table 4 - Reaction conditions used for the qRT-PCR.

Reaction step	Temperature/°C	Time/seconds	Number of cycles
Enzyme activation	95	900	1
Denaturation	94	15	39
Annealing	Annealing temperature (primer specific)	20	
Extension	72	20	
Melting curve	65 to 95	5	1

2.4 Histological analysis

2.4.1 Thymic morphology

For histological analysis, the collected thymi from WT animals, induced or not with EAE, were embedded in paraffin and sectioned at 4μm. The paraffin sections were then stained with hematoxylin and eosin (HE), for the visualization of the cell's nucleus and cytoplasm, respectively.

2.4.2 Immunofluorescence for GFAP

Brains collected at the sacrifice, during the onset and chronic phases, were sectioned at 20μm (coronal sections) and cerebellum sections were further selected and stained for GFAP, in order to evaluate astrogliosis present in the cerebellar white matter. Sections were fixed in 4% PFA in PBS for 30 minutes at RT. After antigen retrieval, with citrate buffer (C9999; Sigma-Aldrich®) in the microwave for 20 minutes, the tissue was permeabilized with PBS-Triton 0.3% at RT for 10 minutes and subsequently blocked with 10% fetal bovine serum (FBS) in PBS-triton 0.3% at RT for 30 minutes. For the immunofluorescent staining for GFAP, slides were incubated overnight with rabbit anti-mouse GFAP antibody (1:200; Dako, Denmark), diluted in PBS-triton 0.3% with 10% of FBS. The respective secondary fluorescent antibody Alexa Fluor® 594 donkey anti-rabbit (A21207; Life Technologies) diluted 1:500 in PBS-triton 0.3% was used for 2 hours at RT. Next, the slides were incubated with DAPI (1:200; Invitrogen, Life Techologies), cover-slipped with Immumount (99-904; Fisher Scientific, Thermo Fisher Scientific) and examined under fluorescent light. To quantify the total GFAP+ area, photographs were taken in 20 non-overlapping fields of the cerebellar white matter, using a fluorescent microscope (BX61,

Olympus, Hamburg, Germany), and analysed using the Fiji software (Schindelin et al., 2012). For each animal, it was calculated the average of GFAP+ area in the total number of photographs.

2.4.3 Luxol Fast Blue

The histochemical staining Luxol Fast Blue was used to evaluate lesioned sites, with inflammatory infiltrates, in the cerebellum. Selected frozen sections of cerebellum were fixated in 95% ethanol at RT for 15 minutes, and stained in 0.1% luxol fast blue MBS (1B-389; Chroma-Gesellshaft, Schmidt Gmbh+Co, Köngen, Germany) in 0.5% glacial acetic acid with 95% ethanol solution, over-night at 56°C. The excess of dye was removed using first 95% ethanol and then running water. Slides were differentiated with 0.05% lithium carbonate (62470; Sigma-Aldrich®) for 10 minutes and with 70% ethanol for 10 seconds, counterstained with hematoxylin, dehydrated and mounted with Entellan® (107961; Merck Millipore).

The quantification of demyelination was done in representative sections of the entire cerebellum (minimum of 7 cerebellum sections examined per animal), using an Olympus microscope and the Stereo Investigator software (MBF Bioscience, Williston, Vermont, USA). The total white matter area was drawn using an objective of 4x and the demyelination areas were delimitated using the objective of 10x. The percentage of demyelination was determined by dividing the sum of the demyelination areas by the total white matter area, multiplied by 100.

2.5 Serum corticosterone quantification

Blood was collected during the sacrifice and was posteriorly centrifuged, for 10 minutes at 13000rpm, and serum was collected and stored at -80°C. Subsequent corticosterone quantification was performed using a commercial ELISA kit (ADI-901-097; Enzo Life Sciences, Inc., Farmingdale, NY, USA), according to the manufacturer's instructions. Briefly, samples were incubated with a specific antibody for corticosterone and a known concentration of corticosterone labelled with alkaline phosphatase, which competed with the sample corticosterone for the binding sites of the antibodies. After washing the unspecific binding, a substrate of alkaline phosphatase was added to the wells and the reaction originated a coloured solution. The optical density (OD) of the wells was read using a Microplate Reader (Model 680, BioRad Laboratories). The samples corticosterone concentration was calculated using the GraphPad Prism 6.0 (GraphPad Software, Inc., La Jolla, CA, USA), after fitting a 4 parameter logistic curve to the standards ODs.

2.6 Statistical analysis

Results were analysed using GraphPad Prism 6.0, and statistical significance was considered for $p<0.05$. In the first set of results, where we aimed to address the thymic response only in WT mice, to compare different WT groups (non-induced, EAE onset and EAE chronic) a one-way ANOVA was used. In the second set of results, to compare WT and LCN2-null mice, non-induced or at the onset or chronic phases of EAE a two-way ANOVA was used. To compare disease measurements (day of first score, day of score=3, first score different from 0) between EAE LCN2-null and WT mice a t-test for independent samples was used. The Kolmogorov-Smirnov test was used to test the normality of the distribution of the samples. When a suitable non-parametric test was not available a parametric test was used, even if the samples did not presented a normal distribution. Differences between groups were determined by Bonferroni's multiple comparison test post hoc analysis. All values are expressed as mean±SEM and as the average of all the experiments performed.

3. RESULTS

3. RESULTS

3.1 Chronic disease course in MOG_{35-55} induced EAE

After EAE induction with MOG_{35-55} WT animals developed a chronic disease course, with the first symptoms appearing at around day 11 (Figure 6A), coincidently with the beginning of weight loss by these animals (Figure 6B). The EAE animals lost about 20% of their initial weight between days 11 and 17, which is when the chronic phase of disease begins. At day 16 the disease was at the peak of activity, while at day 23 the animals were already in a chronic phase, which is why these timepoints were chosen as endpoints for the experiments.

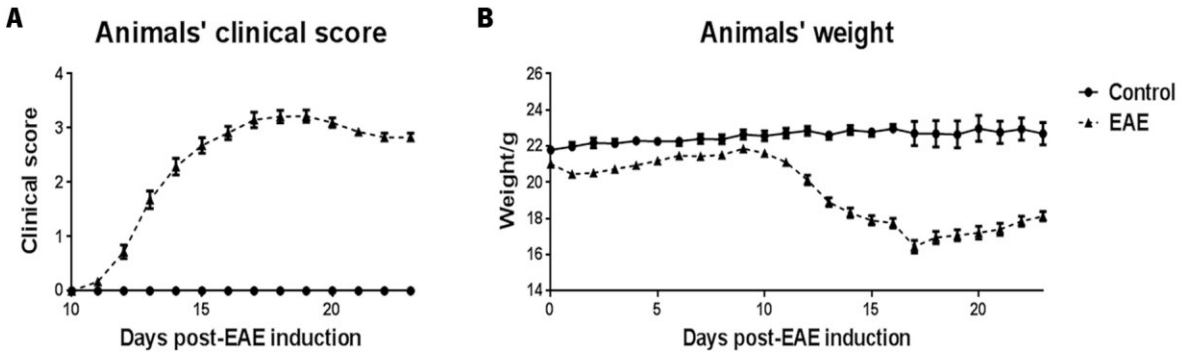

Figure 6 - *Disease course of MOG_{35-55}-induced EAE in WT animals.* EAE WT animals induced with MOG_{35-55} presented the first symptoms at day 11 post-disease induction, at around day 16 the disease reached a peak of activity, and after that the animals remained with a similar score until the end of the experiment, at day 23 (chronic phase of disease) (A). The EAE animals started losing weight after the appearance of the first symptoms, at day 11 (B). (From day 0 to day 16 post-EAE induction: $n_{non\text{-}induced}$=37, n_{EAE}=46; from day 17 to day 23 post-EAE induction: $n_{non\text{-}induced}$=10, n_{EAE}=15. Data presented as mean±SEM).

3.2 The proportion of the four main populations of the thymus was altered in WT animals during the onset phase EAE but was restored in the chronic phase of disease

To assess alterations in the thymus populations during the EAE course we collected the animals' thymi during the sacrifice and performed flow cytometry in WT animals induced with EAE, and used non-induced animals as controls. Animals were sacrificed at the onset and chronic phases of disease. The EAE animals presented thymic atrophy, at both timepoints, as assessed by thymus weight, normalized for total body weight (non-induced=0.002218±0.0000996, EAE onset=0.000532±0.0001433, EAE chronic=0.000655±0.0001631; $F_{(2,12)}$=46.48, $p<0.0001$) (Figure 7A), and total cell number (non-induced=10.92±0.625x10^7, EAE onset=2.09±0.932x10^7, EAE chronic=2.52±0.502x10^7, $F_{(2,40)}$=50.58,

p<0.0001) (Figure 7B). Also the percentage of viable cells, evaluated by lack of 7-ADD staining and counted in the MUSE® cell analyser, was decreased in EAE animals (non-induced=86.80±1.571, EAE onset=77.79±1.891, EAE chronic=76.79±3.167, $F_{(2,40)}$=7.914, p=0.0013) (Figure 7C).

Thymocytes were stained for CD3, CD4 and CD8, to distinguish the 4 main populations present in the thymus, namely the DN, DP and single positive, for CD4 or CD8, populations. A representative CD4 *vs.* CD8 plot for each of the groups analysed is presented in Figure 7D. During the onset phase of disease the percentage of the four populations was altered, having occurred a significant decrease in the DP cells (non-induced=83.27±0.747, EAE onset=27.24±8.039, EAE chronic=68.29±7.705, $F_{(2,40)}$=29.95, p<0.0001), and an increase in both single positive populations (CD4+CD8-: non-induced=6.63±0.411, EAE onset=40.63±5.171, EAE chronic=8.34±2.990, $F_{(2,40)}$=36.84, p<0.0001; CD4-CD8+: non-induced=1.42±0.114, EAE onset=7.76 ±1.466, EAE chronic=2.763±1.466, $F_{(2,40)}$=13.53, p<0.0001). The percentage of these populations was re-established to control levels in the chronic phase. Regarding the DN population there was an increase along disease development (non-induced=2.12±0.161, EAE onset=8.98±1.095, EAE chronic=10.05±2.836, $F_{(2,40)}$=12.04, p<0.0001) (Figure 7E).

As for the absolute numbers of the four populations, they were decreased in EAE animals, at both timepoints, when compared to non-induced mice, which could be a consequence of the decrease in the total cell number (DN: non-induced=2.32±0.240x10^6, EAE onset=1.13±0.208x10^6, EAE chronic=1.77±0.394x10^6, $F_{(2,40)}$=5.511, p=0.0077; DP: non-induced=90.99±5.453x10^6, EAE onset=12.00±8.202x10^6, EAE chronic=19.28±4.292x10^6, $F_{(2,40)}$=51.08, p<0.0001; CD4+CD8-: non-induced=6.91±0.404x10^6, EAE onset=4.65±0.621x10^6, EAE chronic=1.46±0.416x10^6, $F_{(2,40)}$=27.67, p<0.0001; CD4-CD8+: non-induced=1.45±0.080x10^6, EAE onset=0.90±0.143x10^6, EAE chronic=0.36±0.112x10^6, $F_{(2,40)}$=23.09, p<0.0001) (Figure 7F). Interestingly, although in the chronic phase of disease the total cell numbers were decreased, like in the onset phase, there was a re-establishment of the proportions between the four populations to the levels of non-induced animals.

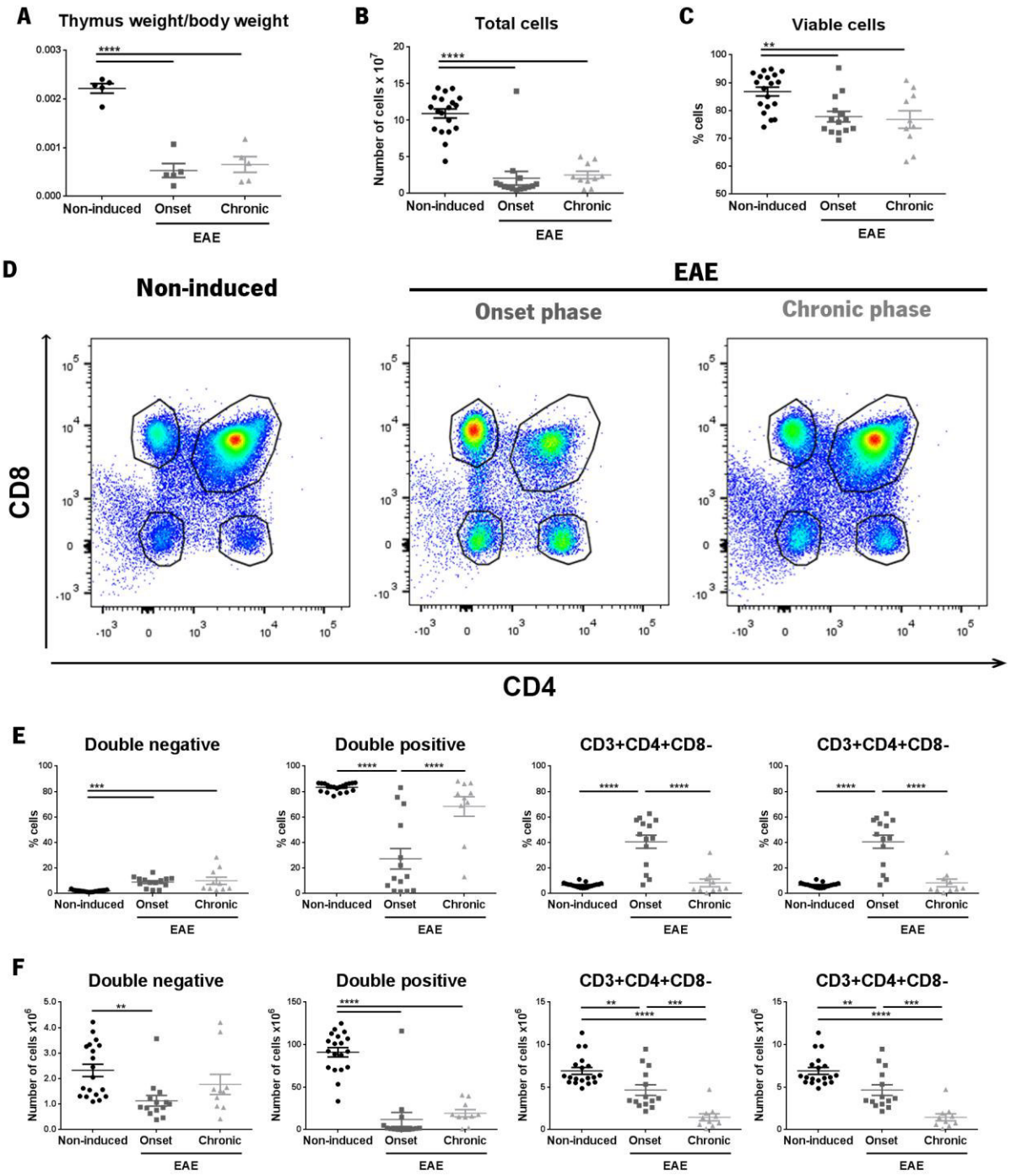

Figure 7 – *Thymus flow cytometry results.* Animals induced with EAE presented thymic atrophy, as assessed by the thymus weight, normalized for total body weight (A), and the total cell number per µL, counted in the MUSE® cell analyser (B). The percentage of viable cells was decreased in EAE animals (C). Representative CD4 *vs.* CD8 plots of the control group (left D) and EAE groups, at the onset phase of disease (middle D) and chronic phase (right D), showed differences in thymocyte populations between the groups. The percentage of double positive cells decreased at the onset of disease, while the percentage of both CD4 and CD8 single positive populations increased, compared with non-induced animals. At the chronic phase of disease the percentage of these populations was restored to the levels of non-induced animals. The percentage of double negative cells increased with disease development (E). The total cell number per µL of all populations decreased along disease development, which could be a consequence of the decreased total cell number (F). ($n_{non\text{-}induced}$=19, $n_{EAE\ onset}$=14, $n_{EAE\ chronic}$=10. Data presented as mean±SEM. *p<0.05, **p<0.01, ***p<0.001, ****p<0.0001).

3.2.1 Corticosteroid measurement

Previous studies have reported that the activation of the hypothalamic-pituitary-adrenal (HPA) axis, during stressful stimuli or pathological conditions can induce thymic atrophy, characterized mainly by acute loss of cortical DP thymocytes. (Gruver & Sempowski, 2008). For that reason, we next quantified corticosterone concentration in the serum of the animals, at the day of sacrifice. The corticosterone levels although not significantly different, tend to be higher in EAE induced mice compared with non-induced mice (non-induced=23.05±2.479, EAE onset=41.40±10.330, EAE chronic=34.84±7.179, $F_{(2,12)}$=1.579, p=0.2461) (Figure 8).

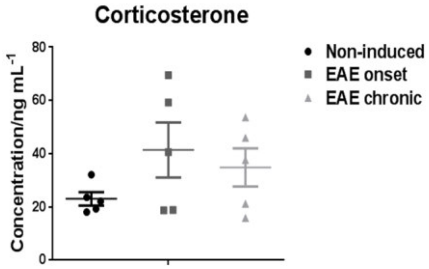

Figure 8 – *Corticosterone serum concentration at the sacrifice day.* EAE animals, at both timepoints, did not present statistically significant increased levels of corticosterone at the day of sacrifice. ($n_{non\text{-}induced}$=5, $n_{EAE\ onset}$=5, $n_{EAE\ chronic}$=5. Data presented as mean±SEM).

3.3 Thymic histological morphology was altered in WT EAE animals

The thymus is morphologically divided in cortex and medulla, which are separated by a vascular corticomedullary zone. After observing a decrease in the percentage of DP cells, during the onset phase of disease, we next went to assess the consequences in thymic morphology. Macroscopically, the thymi of WT EAE animals were decreased in size, resulting in a decreased weight, even after normalization for total body weight (Figure 7A), when compared to non-induced animals. In non-induced animals, the thymus presented a normal morphology, with clearly distinctive areas of cortex and medulla (Figure 9, left panel). In WT EAE animals, in the initial phases of disease development when they present lower clinical scores (clinical score=1), although the decrease in the thymus weight, the thymic morphology is still similar to non-induced animals, being possible the distinction between areas of cortex and medulla (Figure 9, middle panel), while in more advanced stages of the disease, when the animals are already paralyzed (clinical score=3), the medulla is almost inexistent (Figure 9, right panel).

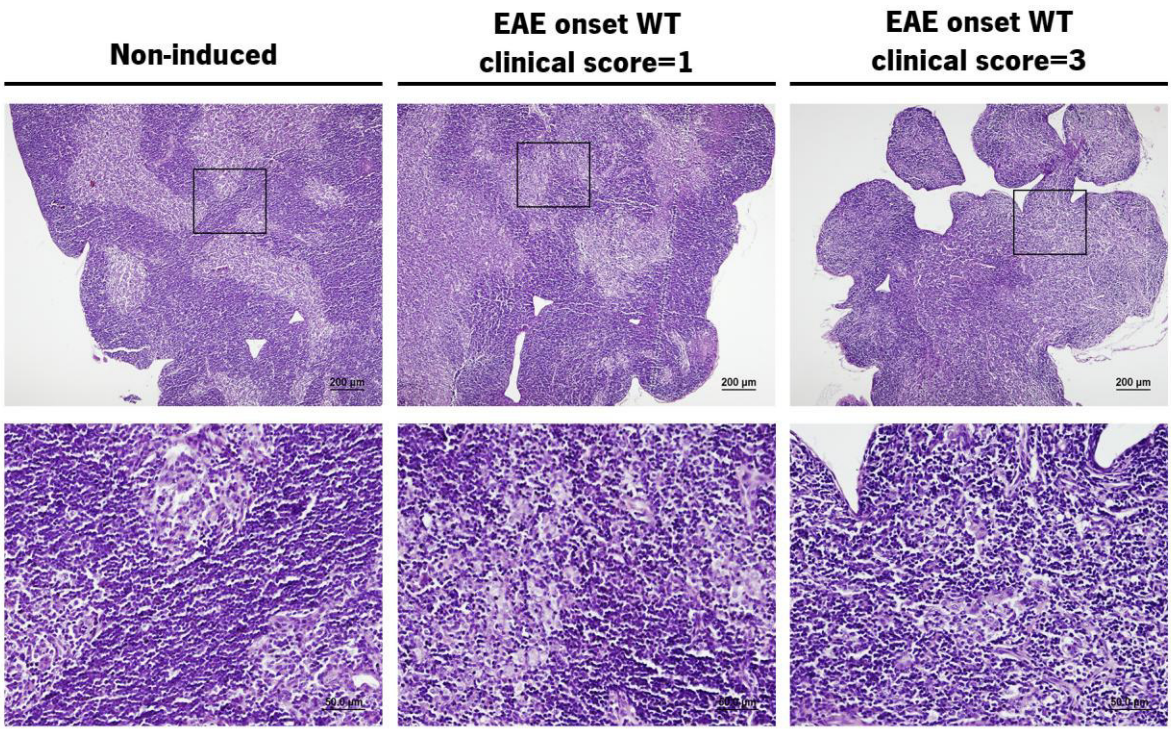

Figure 9 – *Histological morphology of the thymus in WT non-induced and EAE animals at the onset phase of disease*. Non-induced animals present a normal histological morphology of the thymus, with distinct areas of cortex and medulla. In EAE animals, at earlier stages of disease the morphology is similar to non-induced animals, while in later stages the areas of medullary tissue is scarce (upper panel bar=200µm; lower panel bar=50µm).

3.4 Disease course in LCN2-null mice was similar to WT animals

EAE was induced in LCN2-null mice with the same protocol used for WT animals. We did not observe significant differences between LCN2-null and WT mice in overall disease development (Figure 10A), nor in specific disease measurements, such as the mean day when the animals presented the first symptoms, the mean day when they reached a clinical score of 3, i.e., when the animals became paralyzed, and the mean first score of disease given to the animals (Table 5). Also, the body weight variances along the experiment were similar in both genotypes (Figure 10B). Regarding disease incidence, only one animal of each genotype did not develop disease symptoms, and they were subsequently excluded from all the analysis.

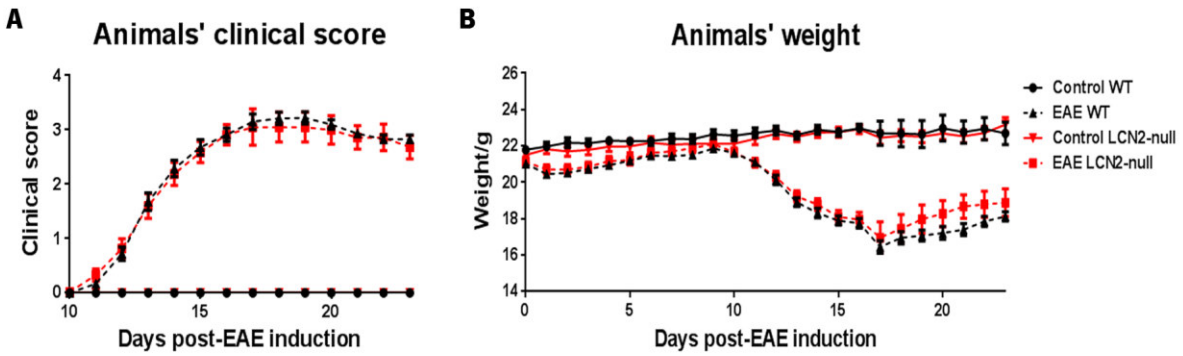

Figure 10 – *Disease course of MOG_{35-55}-induced EAE in LCN2-null mice and WT littermates.* In LCN2-null mice the disease course is similar to WT littermates, with no significant differences between the clinical scores of both genotypes (A). LCN2-null EAE mice also lose weight in a similar way as the WT EAE animals (B). (From day 0 to day 16 post-EAE induction: $n_{non\text{-}induced\ WT}$=37, $n_{EAE\ WT}$=46, $n_{non\text{-}induced\ LCN2\text{-}null}$=38, $n_{EAE\ LCN2\text{-}null}$=37; from day 17 to day 23 post-EAE induction: $n_{non\text{-}induced\ WT}$=10, $n_{EAE\ WT}$=15; $n_{non\text{-}induced\ LCN2\text{-}null}$=15, $n_{EAE\ LCN2\text{-}null}$=11. Data presented as mean±SEM).

Table 5 – EAE progression in LCN2-null mice and WT littermate mice.

	Incidence	Day of 1st symptoms (n)	Day of clinical score=3 (n)	1st clinical score (higher than 0) (n)
WT	37/38	12.35±0.170 (37)	14.65±0.220 (31)	1.08±0.091 (37)
LCN2-null	28/29	12.43±0.319 (28)	14.52±0.332 (23)	0.89±0.099 (28)
t test value		$t_{(63)}$=0.2279	$t_{(52)}$=0.3220	$t_{(63)}$=1.6416
p value		0.8205	0.7487	0.1057

3.5 LCN2-null mice presented similar alterations to the WT animals regarding thymic populations, during EAE development

The thymi of LCN2-null mice were processed for flow cytometry analysis the same way as for WT animals, to evaluate if LCN2 absence influences the thymic response in the context of EAE. LCN2-null mice present similar CD4 *vs.* CD8 plots to the WT animals, both for the non-induced animals and for the EAE animals, at the onset and chronic phases of disease (Figure 11A). The percentage of CD4 and CD8 single positive cells increased in LCN2-null mice at the onset phase of disease, and was restored to the levels of non-induced animals at the chronic phase, while the percentage of DN increased along disease progression. As for the percentage of DP cells, it decreased at the onset phase and increased again at the chronic phase. Of notice, the percentage of DP cells in the LCN2-null mice during the chronic phase was still significantly lower than non-induced animals (Table 6 and Figure 11B). The LCN2-null EAE animals presented a decrease in the cell number of all thymocyte populations, at both phases of EAE, except for the DN cells, similarly to what happed in WT animals (Table 7 and Figure

11C).To sum up, for both the thymus cell numbers and percentages, we only observed a significant effect of the disease factor, with neither the genotype nor the interaction between factors presenting a significant influence in the thymic populations (Tables 6 and 7).

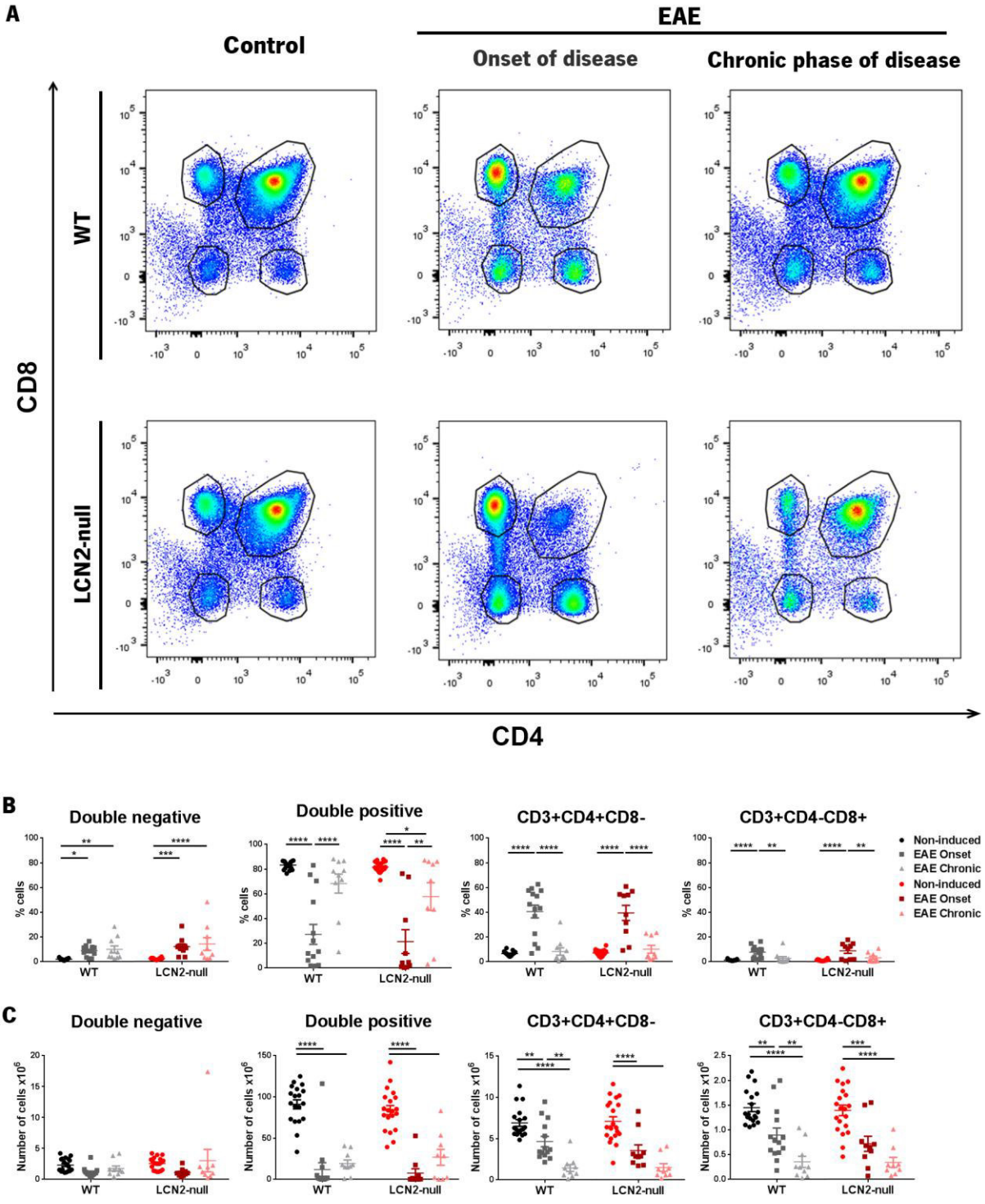

← **Figure 11 –** *Flow cytometry results in LCN2-null and WT mice.* Representative CD4 *vs.* CD8 plots of the WT control group (left up A), WT onset (middle up A), WT chronic (right up A), LCN2-null control (left down A), LCN2-null onset (middle down A) and LCN2-null chronic (middle down A). Flow cytometric analysis of the LCN2-null mice thymus shows similar results to the WT animals, indicating that the lack

of LCN2 does not influence thymocytes number (B) nor the thymus populations percentages (C) during EAE development ($n_{non\text{-}induced\ WT}$=19, $n_{EAE\ onset\ WT}$=14, $n_{EAE\ chronic\ WT}$=10, $n_{non\text{-}induced\ LCN2\text{-}null}$=20, $n_{EAE\ onset\ LCN2\text{-}null}$=11, $n_{EAE\ chronic\ LCN2\text{-}null}$=10. Data presented as mean±SEM. *p<0.05, **p<0.01, ***p<0.001, ****p<0.0001).

Table 6 - Two-Way ANOVA results for the comparison of thymus population's percentages between LCN2-null and WT mice.

				Mean±SEM	Disease factor	Genotype factor	Interaction
Percentage of cells	DN	WT	Non-induced	2.12±0.161	$F_{(2,76)}$=42.70, p<0.0001	$F_{(1,76)}$=0.7023, p=0.4046	$F_{(2,76)}$=0.2194, p=0.8035
			EAE onset	8.98±1.095			
			EAE chronic	10.05±2.836			
		LCN2-null	Non-induced	2.49±0.143			
			EAE onset	12.14±2.252			
			EAE chronic	14.27±5.136			
	DP	WT	Non-induced	83.27±0.747	$F_{(2,76)}$=53.54, p<0.0001	$F_{(1,76)}$=1.441, p=0.2337	$F_{(2,76)}$=0.2764, p=0.7593
			EAE onset	27.24±8.039			
			EAE chronic	68.29±7.705			
		LCN2-null	Non-induced	81.61±0.958			
			EAE onset	21.43±9.635			
			EAE chronic	57.81±11.200			
	CD3+CD4+CD8-	WT	Non-induced	6.63±0.411	$F_{(2,76)}$=66.91, p<0.0001	$F_{(1,76)}$=0.0144, p=0.9049	$F_{(2,76)}$=0.0926, p=0.9117
			EAE onset	40.63±5.171			
			EAE chronic	8.34±2.990			
		LCN2-null	Non-induced	7.157±0.559			
			EAE onset	39.36±6.103			
			EAE chronic	10.04±3.165			
	CD3+CD4-CD8+	WT	Non-induced	1.42±0.114	$F_{(2,76)}$=27.02, p<0.0001	$F_{(1,76)}$=0.4995, p=0.4819	$F_{(2,76)}$=0.1983, p=0.8205
			EAE onset	7.76±1.288			
			EAE chronic	2.76±1.466			
		LCN2-null	Non-induced	1.43±0.126			
			EAE onset	8.96±2.057			
			EAE chronic	3.35±1.296			

Table 7 – Two-Way ANOVA results for the comparison of thymus cell numbers between LCN2-null and WT mice.

				Mean±SEM ($x10^6$)	Disease factor	Genotype factor	Interaction
Number of cells	DN	WT	Non-induced	2.32±0.240	$F_{(2,76)}$=3.639, p=0.031	$F_{(1,76)}$=1.165, p=0.2838	$F_{(2,76)}$=0.6266, p=0.5372
			EAE onset	1.13±0.208			
			EAE chronic	1.77±0.394			
		LCN2-null	Non-induced	2.56±0.218			
			EAE onset	1.11±0.204			
			EAE chronic	3.05±1.810			
	DP	WT	Non-induced	90.99±5.453	$F_{(2,76)}$=88.74, p<0.0001	$F_{(1,76)}$=0.0512, p=0.8217	$F_{(2,76)}$=0.5807, p=0.5620
			EAE onset	12.00±8.202			
			EAE chronic	19.28±4.292			
		LCN2-null	Non-induced	83.92±5.635			
			EAE onset	7.71±5.297			
			EAE chronic	26.79±9.683			
	CD3+CD4+CD8-	WT	Non-induced	6.91±0.404	$F_{(2,76)}$=48.51, p<0.0001	$F_{(1,76)}$=0.3561, p=0.5524	$F_{(2,76)}$=0.7636, p=0.4695
			EAE onset	4.65±0.621			
			EAE chronic	1.46±0.416			
		LCN2-null	Non-induced	7.10±0.562			
			EAE onset	3.56±0.691			
			EAE chronic	1.50±0.467			
	CD3+CD4-CD8+	WT	Non-induced	1.45±0.080	$F_{(2,76)}$=42.70, p<0.0001	$F_{(1,76)}$=0.7023, p=0.4046	$F_{(2,76)}$=0.2194, p=0.8035
			EAE onset	0.90±0.143			
			EAE chronic	0.35±0.112			
		LCN2-null	Non-induced	1.39±0.105			
			EAE onset	0.71±0.152			
			EAE chronic	0.34±0.100			

3.5.1 Corticosteroid measurements

Unlike to what happened in WT animals, at the onset phase of disease, the LCN2-null mice showed an increase in the serum levels of corticosterone, but at the chronic phase these levels were re-established to the levels of non-induced animals (Figure 12). Also, during the onset phase, the corticosterone levels were significantly higher in LCN2-null mice compared with WT animals at the same phase of disease (non-induced WT=23.05±2.479, EAE onset WT=41.40±10.330, EAE chronic WT=34.84±7.179, non-induced LCN2-null=27.70±8.026, EAE onset LCN2-null=76.46±11.670, EAE chronic LCN2-null=37.93±13.500; disease factor: $F_{(2,23)}$=7.073, p=0.004, genotype factor: $F_{(1,23)}$=3.554, p=0.0721, interaction: $F_{(2,23)}$=1.925, p=0.1687) (Figure 12).

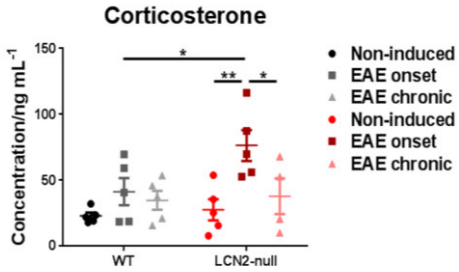

Figure 12 – *Serum corticosterone concentration in LCN2-null and WT mice at the sacrifice day.* At the onset of disease EAE LCN2-null mice present increased levels of corticosterone, compared with control LCN2-null mice and WT mice at the onset of disease, at the sacrifice day. ($n_{non\text{-}induced\ WT}$=5, $n_{EAE\ onset\ WT}$=5, $n_{EAE\ chronic\ WT}$=5, $n_{non\text{-}induced\ LCN2\text{-}null}$=5, $n_{EAE\ onset\ LCN2\text{-}null}$=5, $n_{EAE\ chronic\ LCN2\text{-}null}$=5. Data presented as mean±SEM. *p<0.05, **p<0.01).

3.6 LCN2 deficiency results in a decreased inflammatory profile in the cerebellum of EAE animals

Clinical studies have shown relevant cerebellar deficits in MS patients (Weinshenker et al., 1996). The cerebellum is mainly involved in coordination and balance, thus playing an important role in the modulation of movement. (MacKenzie-Graham et al., 2009). Also, even though most studies using the EAE animal model are focused primarily on disease in the spinal cord, the cerebellum has also been shown to be affected in this model (Kuerten et al., 2007; MacKenzie-Graham et al., 2006; MacKenzie-Graham et al., 2009). For this reason we intended to characterize the inflammatory profile in the cerebellum of LCN2-null and WT mice, by quantifying the expression levels of inflammatory cytokines, especially of genes involved in the Th1 and Th17 response, and the percentage of inflammatory infiltrates in the white matter.

3.6.1 Inflammatory cytokines expression levels

The expression levels of inflammatory cytokines involved in the Th1 immune response, namely *Ifn-gamma* (Figure 13A) and *Il12a* (Figure 13B), were increased in the cerebellum of EAE animals, during the onset phase of disease, and decreased in the chronic phase, in both genotypes. Of relevance, the increase in the expression level of *Ifn-gamma* in the LCN2-null mice was less expressive than in the WT mice, being this difference statistically significant. As for *Il17a* (Figure 13C), a cytokine involved in the Th17 response, its expression levels only increased significantly in the onset phase of disease in WT animals, and not in the onset phase of LCN2-null mice. Besides this, during the onset phase, and considering all these three genes, their expression levels is decreased in LCN2-null mice when comparing with WT animals (Figure 13A, B and C), which suggests a decrease in the Th1 and Th17

inflammatory responses in the cerebellum of LCN2-null mice, compared with WT animals. The expression levels of *Il4*, a cytokine produced by Th2 cells, was not different between EAE and non-induced animals (Figure 13D). The results of the two-way ANOVA analysis are presented in Table 8.

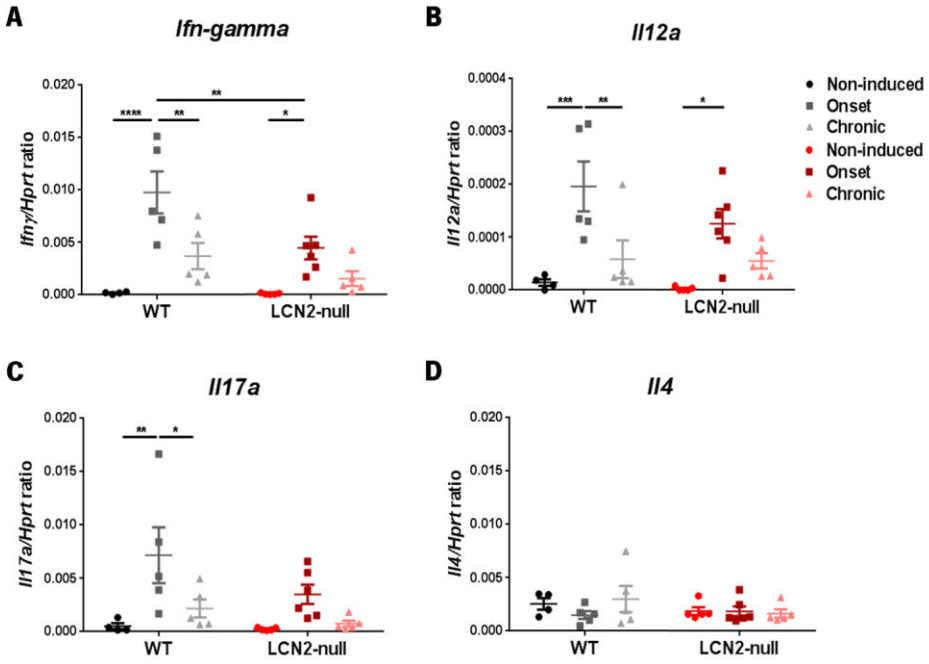

Figure 13 - *Expression levels of inflammatory cytokines in the cerebellum.* During the onset phase of disease, the expression levels of *Ifn-gamma* (A) and *Il12a* (B), which are involved in the Th1 response, are significantly increased in both WT and LCN2-null mice, when compared to non-induced animals. At the chronic phase the expression of these cytokines decreased to the levels of non-induced animals. In the case of *IL17a*, involved in the Th17 response, it was only significantly elevated in the onset phase of disease in the WT animals (C). The expression levels of *Il4*, a cytokine involved in the Th2 response, were not altered (D). ($n_{non\text{-}induced\ WT}$=4, $n_{EAE\ onset\ WT}$=5, $n_{EAE\ chronic\ WT}$=5, $n_{non\text{-}induced\ LCN2\text{-}null}$=5, $n_{EAE\ onset\ LCN2\text{-}null}$=6, $n_{EAE\ chronic\ LCN2\text{-}null}$=5. Data presented as mean±SEM. *p<0.05, **p<0.01, ***<0.001, ****p<0.0001).

Table 8 - Results of the two-way analysis of gene expression in the cerebellum.

			Mean±SEM	Disease factor	Genotype factor	Interaction
Ifn-gamma	WT	Non-induced	2.21e-4±7.08e-5	$F_{(2,24)}$=19.22, p<0.0001	$F_{(1,24)}$=7.180, p=0.0131	$F_{(2,24)}$=2.647, p=0.0914
		EAE onset	9.75e-3±1.998e-3			
		EAE chronic	3.69e-3±1.252e-3			
	LCN2-null	Non-induced	9.40e-5±3.042e-5			
		EAE onset	4.45e-3±1.076e-3			
		EAE chronic	1.54e-3±7.09e-4			
Il12a	WT	Non-induced	1.44e-5±6.25e-6	$F_{(2,24)}$=15.09, p<0.0001	$F_{(1,24)}$=1.471, p=0.2369	$F_{(2,24)}$=0.8521, p=0.4390
		EAE onset	1.96e-4±4.70e-5			
		EAE chronic	5.85e-5±3.550e-5			
	LCN2-null	Non-induced	2.46e-6±1.666e-6			
		EAE onset	1.26e-4±2.78e-5			
		EAE chronic	5.53e-5±1.451e-5			
Il17a	WT	Non-induced	5.19e-4±2.764e-4	$F_{(2,24)}$=9.343, p=0.0010	$F_{(1,24)}$=3.196, p=0.0865	$F_{(2,24)}$=1.010, p=0.3790
		EAE onset	7.16e-3±2.606e-3			
		EAE chronic	2.18e-3±8.39e-4			
	LCN2-null	Non-induced	2.47e-4±5.51e-5			
		EAE onset	3.50e-3±9.03e-4			
		EAE chronic	7.56e-4±2.830e-4			
Il4	WT	Non-induced	3.07e-3±9.20e-4	$F_{(2,24)}$=0.6162, p=0.5483	$F_{(1,24)}$=1.111, p=0.3023	$F_{(2,24)}$=0.9579, p=0.3979
		EAE onset	1.50e-3±3.70e-4			
		EAE chronic	3.00e-3±1.235e-3			
	LCN2-null	Non-induced	1.88e-3±3.62e-4			
		EAE onset	1.86e-3±4.56e-4			
		EAE chronic	1.65e-3±3.87e-4			

3.6.2 Inflammatory infiltrates in the cerebellum white matter

To evaluate lesion areas in the white matter we stained representative sections of the whole cerebellum with the histochemical coloration luxol fast blue. Representative images of the normal cerebellum of a non-induced animal (left panel), and of an animal induce with EAE (right panel) are presented in Figure 14A. For both the onset and chronic phases of disease, the lesioned areas where identified as areas stained lighter blue with luxol and with the presence of inflammatory infiltrates, in the white matter (Figure 14A, right bottom panel). The sum of lesioned areas was divided by the total white matter area, in order to obtain a measurement of the percentage of lesioned area. Animals from both genotypes presented a decrease in the percentage of lesioned area, in the cerebellum white matter, at the chronic phase of disease, when compared with animals at the onset phase, but this decrease was only

statistically significant for the WT animals (EAE onset WT=4.01±0.766, EAE chronic WT=1.36±0.339, EAE onset LCN2-null=2.62±0.350, EAE chronic LCN2-null=0.65±0.197; disease factor: $F_{(1,30)}$=9.640, p=0.0041, genotype factor: $F_{(1,30)}$=2.052, p=0.1623, interaction: $F_{(1,30)}$=0.251, p=0.6201) (Figure 14B). We also found a high correlation between the percentage of lesioned areas in the cerebellum and the animals' clinical score, during the onset phase of disease, for the WT animals (r=0.7537, r^2=0.5681, p=0.0019), but not for the LCN2-null mice (r=0.5161, r^2=0.2663, p=0.1268) (Figure 14C).

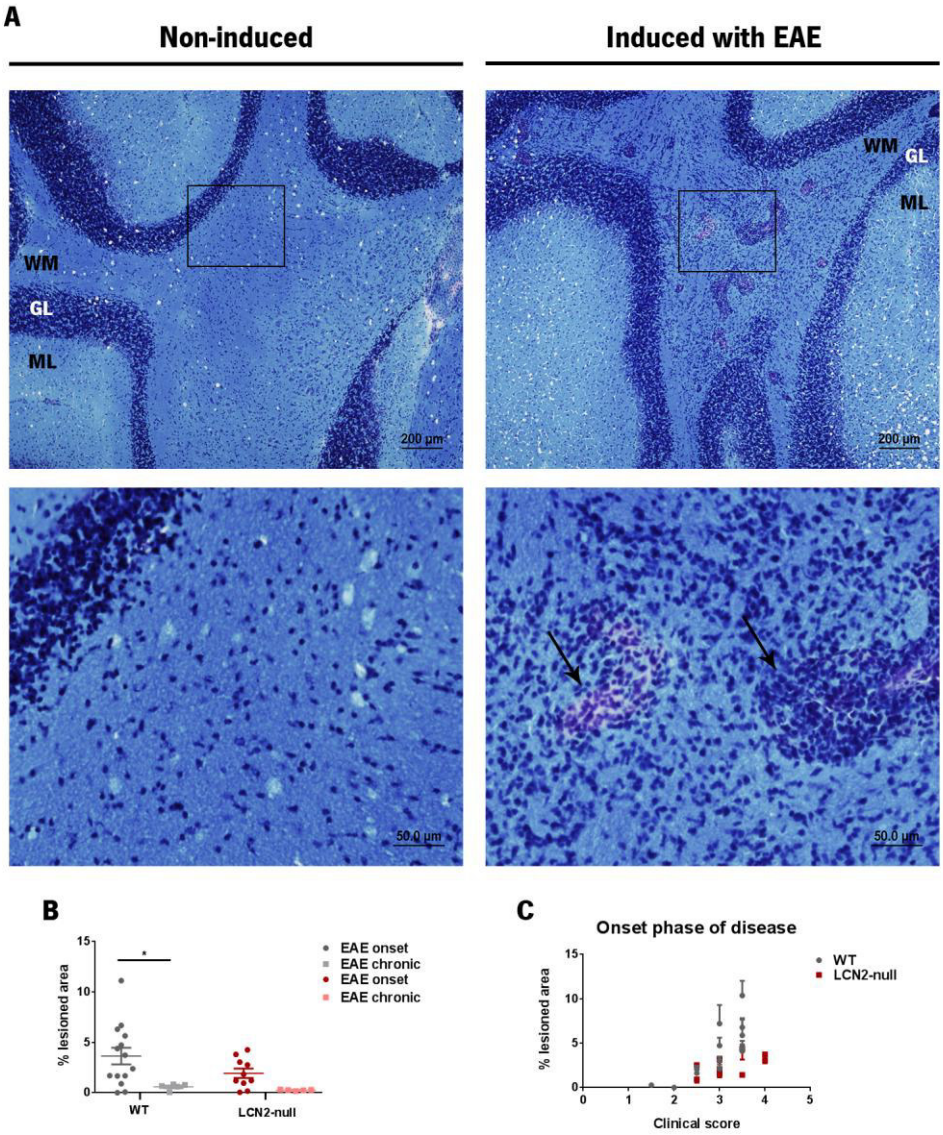

Figure 14 – *Luxol fast blue staining for myelin in cerebellum slices.* The cerebellum white matter of animals induced with EAE present lesion areas which are not seen in control animals. These areas correspond to lesioned areas and are identified after luxol fast blue staining as less blue areas with inflammatory infiltrates (arrows) (upper panel bar=200µm, lower panel bar=50µm) (A). At the chronic phase of disease the percentage of lesioned areas decreases in WT and LCN-2 null EAE animals, compared with the onset phase (B). During the onset phase of disease the percentage of lesioned areas correlates highly with the clinical score in WT animals, but not in LCN2-null mice (C) ($n_{EAE\ onset\ WT}$=14, $n_{EAE\ chronic\ WT}$=5, $n_{EAE\ onset\ LCN2\text{-}null}$=10, $n_{EAE\ chronic\ LCN2\text{-}null}$=5. WM – white matter; ML – molecular layer; GL – granular layer. Data presented as mean±SEM. *p<0.05).

3.7 Astrogliosis is increased in the cerebellum during EAE

Previous studies have shown that, in the context of a relapse-remitting EAE model, astrocytes express LCN2 (Marques et al., 2012), so we evaluated if LCN2 deficiency influences astrocytic activation in the chronic model of EAE. To do so, we stained cerebellum slices for GFAP, and photographed 20 non-overlapping areas of the white matter. The total GFAP+ area was assessed later using the Fiji software, after converting the colour images into binary images. Representative images of the GFAP staining in cerebellar white matter of non-induced animals and animals induced with EAE, at the onset and chronic phases of disease, are presented in Figure 15A. The quantification of the total GFAP+ area showed an increase at the onset and chronic phases of disease, both WT and LCN2-null mice induced with EAE, compared with non-induced animals (non-induced WT=2.46±0.756, EAE onset WT=9.31±1.381, EAE chronic WT=12.52±2.499, non-induced LCN2-null=0.95±0.286, EAE onset LCN2-null=12.00±2.260, EAE chronic LCN2-null=10.55±4.778; disease factor: $F_{(2,12)}$=9.660, p=0.0032, genotype factor: $F_{(1,12)}$=0.018, p=0.8964, interaction: $F_{(2,12)}$=0.539, p=0.5967) (Figure 15B).

We also measured the expression levels of *Gfap* in the cerebellum of WT and LCN2-null mice, in both phases of the disease, and we found an increase in its expression levels at the onset phase of disease, and a decrease to similar levels of non-induced animals during the chronic phase, in both genotypes (non-induced WT=0.0495±0.01408, EAE onset WT=0.2320±0.04622, EAE chronic WT=0.1289±0.02823, non-induced LCN2-null=0.0219±0.00357, EAE onset LCN2-null=0.1883±0.02243, EAE chronic LCN2-null=0.0717±0.01088; disease factor: $F_{(2,24)}$=25.560, p<0.0001, genotype factor: $F_{(1,24)}$=3.732, p=0.0653, interaction: $F_{(2,24)}$=0.328, p=0.7237) (Figure 15C).

Figure 15 – *GFAP immunohistochemical staining and expression levels in the cerebellum.* Representative images from the cerebellum white matter show the presence of astrogliosis in EAE animals during the onset and chronic phases of disease (A), which lead to an increase in the percentage of GFAP positive area in these two phases of disease, both in WT and LCN2-null mice, when compared with non-induced animals (B). The expression levels of *Gfap* in the total cerebellum were elevated during the onset phase of disease, compared with the levels of non-induced animals, and decreased during the chronic phase (C). (GFAP+ area quantification: $n_{\text{non-induced WT}}$=3, $n_{\text{EAE onset WT}}$=3, $n_{\text{EAE chronic WT}}$=3, $n_{\text{non-induced LCN2-null}}$=3, $n_{\text{EAE onset LCN2-null}}$=3, $n_{\text{EAE chronic LCN-2 null}}$=3; *Gfap* expression levels: $n_{\text{non-induced WT}}$=4, $n_{\text{EAE onset WT}}$=5, $n_{\text{EAE chronic WT}}$=5, $n_{\text{non-induced LCN2-null}}$=5, $n_{\text{EAE onset LCN2-null}}$=6, $n_{\text{EAE chronic LCN-2 null}}$=5. Data presented as mean±SEM. Bar=20μm. *p<0.05, **p<0.01, ***p<0.001). →

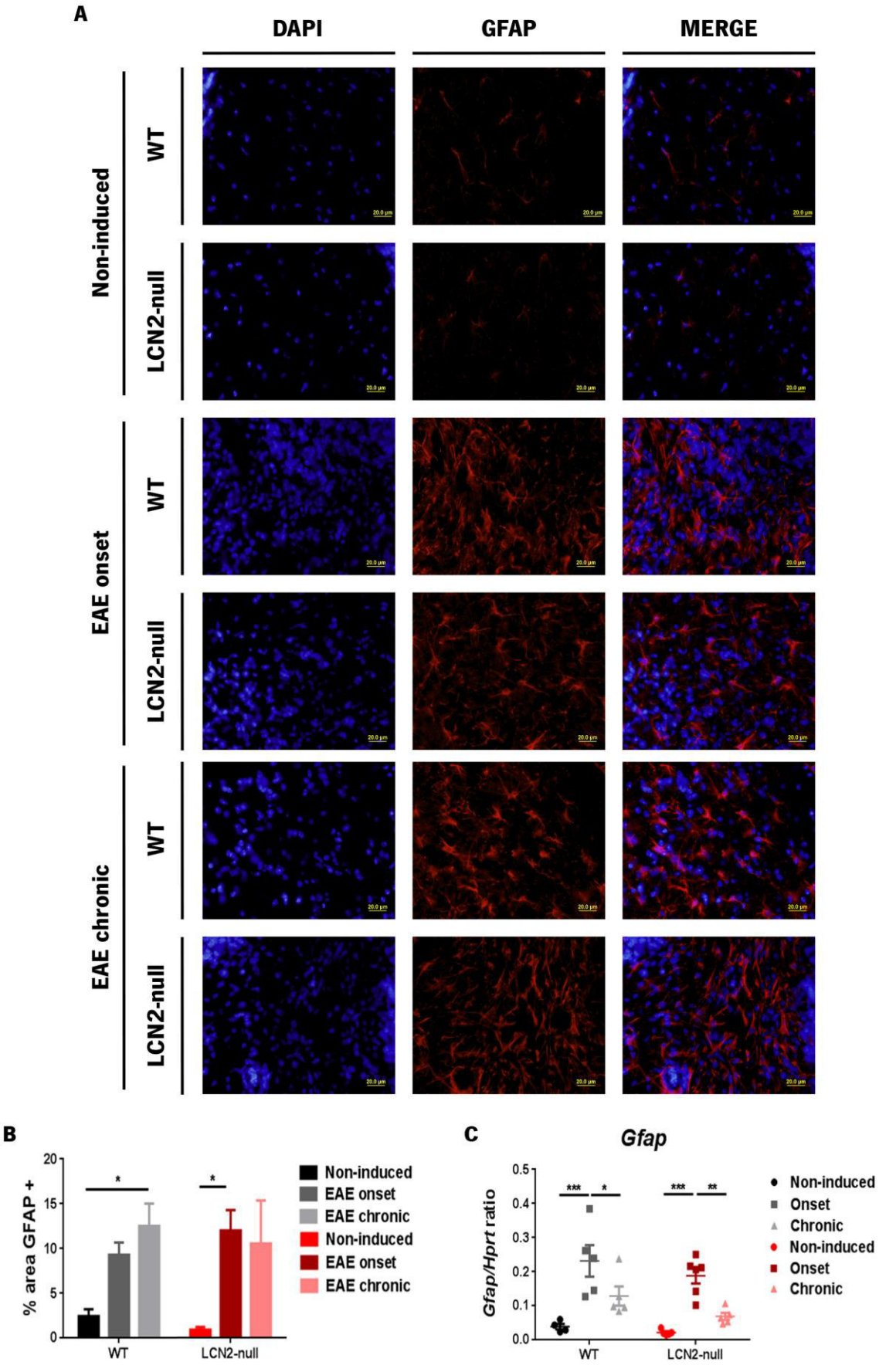
A
DAPI
GFAP
MERGE
Non-induced
EAE onset
EAE chronic
WT
LCN2-null
B
% area GFAP +
Non-induced
EAE onset
EAE chronic
WT
LCN2-null
C
Gfap
Gfap/Hprt ratio
Non-induced
Onset
Chronic
WT
LCN2-null

4. DISCUSSION

4. DISCUSSION

The work presented here was designed to characterize thymic alterations during EAE development, in a chronic model of disease, and also to further explore the role of LCN2 in several aspects of EAE progression.

Using both WT and LCN2-null mice induced with EAE, we were able to show that when the disease in completely established (day 16), in the periphery, the thymus presented altered population proportions, and in the CNS, specifically in the cerebellum, there was increased inflammatory activity, characterized by increase in pro-inflammatory cytokines expression, the presence of inflammatory infiltrates and astrogliosis. At the chronic phase of disease (day 23), although the clinical scores of the animals had not improved, the thymic populations were restored, and inflammation was decreased in the cerebellum.

Regarding the contribution of LCN2 to the EAE establishment and progression, in terms of clinical score we didn't observed differences between LCN2-null mice and WT mice induced with EAE. Also the thymic response in EAE LCN2-null mice, both in day 16 and 23, is similar to the EAE WT animals. However a decreased inflammatory response was observed in the cerebellum of LCN2-null mice induced with EAE, compared with WT EAE animals, especially at the onset phase (day 16).

4.1 Thymus characterization in the context of a chronic EAE model

The thymus is a primary lymphoid organ, where bone marrow derived progenitor cells undergo differentiation and maturation, to originate a functional T cell repertoire (Pearse, 2006). Post-natally, it is composed of thymocytes in various states of differentiation and supporting stromal thymic epithelial cells (Gruver & Sempowski, 2008). The thymus is responsible for the differentiation and production of T helper (CD4+) or T cytotoxic (CD8+) subsets of cells, as well as Treg cells, and for that reason plays an important role both in the initiation and the prevention of auto-immunity mechanisms. Concerning the different populations of the thymus, they can be distinguished by their cell-surface markers, being the CD4 and CD8 markers the most important ones, along with T-cell receptor molecules. In MS it is generally accepted that the disease is the result of an autoimmune response against CNS antigens. Immunological, immunohistochemical and molecular analyses of MS tissue suggest that the development of this disease is driven by a Th1+Th17+ type of inflammatory response, in concert with an autoantibody reaction directed against defined CNS myelin and possibly neuronal components.

Studies both in MS patients and EAE animals have shown evidences of thymic engagement during disease development (Duszczyszyn et al., 2010; Hara et al., 1986). Herein in a chronic EAE model we also showed that the thymus is playing a crucial role in the sense that, among other characteristics, there is thymic atrophy, as assessed by a decrease in total thymus weight, normalized for total body weight, and total number of cells.

Using the CD4/CD8 markers we studied the alterations in thymic populations induced by EAE, at the onset and chronic phases of disease. Of interest, we found a decrease in the percentage of DP cells, and an increase in the percentages of CD4 and CD8 single positive cells, at the onset phase. The proportions of these populations were then restored to the levels of non-induced animals at the chronic phase of disease. Using WT animals induced with recombinant MOG instead of MOG_{35-55}, Litwak and colleagues (2013) observed similar alterations in the DP and single positive thymocytes percentages. These two models differ in the sense that MOG_{35-55} induced EAE is independent of B cells, and the induction with recombinant MOG requires the endocytosis and presentation of the antigen by B cells. In this study, they observed a decrease in DP and an increase in single positive percentages in a more active phase of disease (day 18 post-disease induction), but at the chronic phase of disease they only observed a partial recovery of the DP population (recovery from approximately 20% to 55% by day 45). Since they don't present the results from non-induced animals, it is not possible to evaluate if this recovery was sufficient to re-establish the normal populations' percentages. In our case we saw a recovery, to non-induced animals' levels, of the proportions between the different populations in EAE animals already at day 23 after disease induction. Interestingly, and contrary to our results, they also observed a recovery in DP cell number (Litwak et al., 2013).

To our knowledge, this was the only other study that evaluated the thymus populations, in a chronic model of EAE induced in WT animals, at different timepoints of disease, namely at the peak and chronic phases. Previous studies focused on a single timepoint, to compare differences between genotypes (Gran et al., 2010) or treatments (Siatskas et al., 2012), or on Treg cells function (Chen et al., 2009; Zelenay et al., 2010).

Very different animal models have shown to present thymic atrophy and alterations in thymocyte populations. Namely, an animal model of nutritional deprivation presented a decrease in the absolute numbers of all four thymocyte populations (Howard et al., 1999), similarly to what happens in our model. Besides, in this model, the greatest effect was also observed in the DP population, with a decrease in the relative proportion of this population. As for the relative proportions of the other thymocyte populations, they reported an increase in CD4 single positive cells, similarly to what we have,

but the relative proportions of the DN and CD8 single positive populations were not altered in their model (Howard et al., 1999). Also, after herbicide exposure, animals presented a decrease in thymus weight:body weight ratio and in DP thymocytes number (de la Rosa et al., 2005). In both studies, the elevated serum corticosterone levels resulting from the stressful situation, were suggested as a possible cause for the thymic alterations. For that reason we also quantified corticosterone levels in our animal model.

4.1.1 Influence of the hypothalamic-pituitary-adrenal (HPA) axis in thymic alterations in the EAE animal model induced in WT

The activation of the HPA axis, during stressful stimuli or pathological conditions, can induce thymic alterations. This stress-induced thymic atrophy is characterized mainly by acute loss of cortical DP thymocytes, which is the most represented thymic population. Unlike age-induced thymic atrophy, which cannot be reverted, stress-induced atrophy is usually followed by spontaneous recovery, after the stressor has been removed (Gruver & Sempowski, 2008).

To evaluate if the thymic atrophy observed in WT MOG_{35-55} induced EAE was caused by the increase in corticosterone levels we quantified it in the serum of the animals. Although the corticosterone levels were slightly increased at the onset phase of EAE, these levels were not significantly different from the levels neither of the non-induced animals nor from the ones of EAE animals at the chronic phase of disease. Still, we need to increase the number of animals to confirm these results. Also the serum used for corticosterone quantification was collected at the day of the sacrifice, when the animals were exposed to increased levels of stress. So it would also be important to quantify corticosterone basal levels, in serum collected at the *nadir* and *zenith* phases.

It has previously been shown that both lymphotoxin and estrogen are able to induce thymic atrophy, in adrenalectomized animals, i.e., without the influence of elevated levels of glucocorticoids (Hirahara et al., 1994). Taking this into consideration, and to better understand the role of the HPA axis in the MOG_{35-55}-induced chronic model of EAE, it would be interesting to induce the EAE in the animals, and then treat them with metyrapone or mifepristone, which, respectively, block the corticosterone synthesis and act as steroid receptor antagonist, to assess if thymic alterations previously observed in this model are reverted or maintained. Moreover, in a model of acute endotoxin-induced thymic atrophy, the thymus was found to actively respond to stress by up-regulating cytokine and chemokine gene expression, and down-regulating the expression of genes involved in lymphocyte activation and thymocyte differentiation, which could indicate that the intrathymic gene alterations may also contribute

to thymus atrophy (Billard et al., 2011). So it would also be relevant to study the expression levels of genes involved in the pro-inflammatory response and in thymocyte differentiation, in the thymus in our EAE model.

4.1.2 Histological alterations in the thymus

In a model of EAE induced in Lewis rats, after immunization with homogenized brain tissue, it was possible to observe marked atrophy, and the histological examination revealed severe degeneration of T cells, and infiltration of the thymus by macrophages showing phagocytic activity (Hara et al., 1986). To assess if the alterations in the thymocytes populations would translate into morphological alterations in the thymus, we stained paraffin sections of thymus with HE. We observed a loss of cortico-medullary distinction in EAE animals, during the onset phase of disease, in animals with higher clinical scores (clinical score=3), but not in earlier stages of disease development (score=1). Also, in animals with higher clinical scores, there was an almost complete abrogation of the medulla, resultant from the great decrease in the DP cell population, which is the most abundant population in the thymic medulla. Considering that the proportion of this cell population was restored in the chronic phase of disease, to the levels of non-induced animals, it would be important to evaluate the thymic morphology also during this phase of the disease.

Also, to further explore the morphological alterations that occur in the thymus during EAE development, namely regarding the thymic epithelial cells, it would be important to assess the cortical/medullary ratio, after double staining for cytokeratin (CK)5 and CK8, which are expressed in medullary and cortical epithelial cells, respectively.

4.2 Role of LCN2 in the pathophysiology of EAE

4.2.1 Disease development in LCN2-null mice

The role of LCN2 in different disease models is contradictory, with some authors proposing a beneficial and others detrimental roles of LCN2. Regarding the development of immune complex-mediated inflammatory diseases, such as arthritis and systemic lupus erythromatous, LCN2 was found to play a protective role (Shashidharamurthy et al., 2013). On the other hand, using a model of spinal cord injury, LCN2 played a detrimental role, by contributing to neuronal and astrocyte loss, pro-inflammatory cytokine expression, and immune cell infiltration at the lesion site (Rathore et al., 2011). Specifically

for the EAE model, previous works where EAE was induced in LCN2-null mice also present contradictory results. Berard and coworkers (2012) have reported that LCN2-null mice presented a more severe disease, when compared to WT animals, but, on the other hand, Nam and colleagues (2014) observed a reduced severity and delayed disease course in LCN2-null mice. Our results point to a different direction, indicating that LCN2 deficiency does not influence the clinical score of the animals. Possible explanations for the differences between all these results will be discussed next.

When it comes to the experimental procedure to induce EAE, our protocol is very similar to the protocols used by the two groups mentioned, except for the day of the second PTX injection, which was at day 1 in our case and at day 2 in both the other cases, and for the PTX concentration – we administered 217ng of PTX per animal, while the other studies have administered 200ng per animal (Nam et al., 2014) and 400ng per animal (Berard et al., 2012). A higher concentration of PTX exacerbates the disease course, which could explain the fact that our group and Berard's (2012) had higher scores than Nam and colleagues (2014).

Besides, we used older females (10-16 weeks of age) compared to the ones previously used (7-11 weeks) (Berard et al., 2012; Nam et al., 2014). Age has been shown to alter the disease incidence and severity in EAE models, namely it has been shown that EAE severity decreases with age, in a EAE model induced in female rats using spinal cord homogenate at 3, 8 and 26 months of age (Djikic et al., 2015). Previously, male C57BL/6 mice with 8 months of age, induced with MOG_{35-55}, had presented a worst disease phenotype compared with 6-8 weeks old mice (Matejuk et al., 2005).

It is important to notice that in the study by Berard and coworkers (2012) their conclusions about the increased severity in LCN2-null mice is mainly based in results obtained from animals that developed a relapse-remitting disease course, which is not the case of our model. Specifically for the animals that developed a chronic disease course, they also could not find differences between the mean day of onset disease nor between the mean clinical score at disease peak. They could only find differences between genotypes at the end stage of disease (day 28), when the LCN2-null mice presented a more severe mean clinical score. Our experimental endpoints were at days 16 and 23, so we cannot predict if we would have differences between genotypes at day 28. Also their scoring scale is different than the one used by us – our score of 3 corresponds to their 4 (hind limb paralysis).

In the study by Nam and colleagues (2014), the score progression curve of LCN2-null mice was inferior to the WT mice along the experiment, indicating a less severe phenotype in the null mice. Also, the mean day of disease onset and the maximum score was reduced in LCN2-null mice when compared to WT mice. In their study only 1 LCN2-null mouse, in a total of 12, developed complete hind limb

paralysis, unlike the WT animals, in which 9 out of 12 animals became paralyzed, during the 35 days of experiment. In our case, and referring only to the animals sacrificed at the chronic phase, only 1/15 for the WT animals and 1/11 for the LCN2-null mice did not became paralyzed, which indicates identical severity of the disease in both of our groups. However, we did observed that 5/11 LCN2-null mice recovered the movement in the hind limbs after complete paralysis, against only 3/15 WT mice, which also points towards a more detrimental role of LCN2 in the context of EAE.

4.2.2 Thymus alterations and the HPA axis in LCN2-null mice

The LCN2-null mice presented the same alterations in thymic populations as observed in WT animals, namely, a decrease in all thymocyte populations, at the onset and chronic phases of disease, a decrease of DP cells percentage and an increase in CD4+ and CD8+ single positive cells, at the onset phase, and a reestablishment of these percentages at the chronic phase. But, unlike EAE WT animals, which did not present elevated levels of corticosterone, the LCN2-null mice at the onset phase of EAE presented increased levels of this hormone, as compared with the non-induced animals and the LCN2-null mice at the chronic phase of disease. These results are consistent with the ones obtained in a MBP-induced EAE model, in Lewis rats (MacPhee et al., 1989). This model presented elevated levels of corticosterone just before the onset of paralysis, and the peak of corticosterone was coincident with the maximal clinical score. Besides that, the spontaneous recovery of the animals, from clinical symptoms, occurred when the corticosterone levels were still elevated, which indicated that elevated levels of corticosterone could be involved in EAE recovery. This hypothesis was further supported by the fact that bilateral adrenalectomy before disease induction resulted in a rapid disease development and in 100% of mortality rate. Moreover, the administration of corticosterone to these animals was able to revert this phenotype. It could be that in the LCN2-null mice, after EAE induction, the initial inflammatory response taking place in the CNS contributes to elevate corticosterone levels, which in turn will impair thymic function, preventing the differentiation of new activated cells, and thus act as a protection mechanism. As already discussed previously, we need to increase the number of animals in this analysis, to verify if this also happens in WT animals. The decrease in inflammatory infiltrates in the cerebellum of the LCN2-null animals at the chronic phase of disease is consistent with this protective role of corticosterone.

4.2.3 Inflammation in the cerebellum

Most EAE studies are mainly focused in the alterations that occur in the spinal cord, and only few present data regarding the cerebellum. In our study we wanted to evaluate if the deficiency in LCN2, which is a protein involved in the acute phase response to inflammatory stimuli, would influence the inflammatory response to EAE, in the cerebellum. The importance of Th1 and Th17 cells in EAE development has long been recognized, and indeed we observed an increase in the expression levels of cytokines involved in the Th1 and Th17 responses, namely of *Ifn*-gamma, *Il12a* and *Il17a*, in both the WT and LCN2-null mice, during the onset phase of disease. During the chronic phase, the expression levels of these cytokines decreased. Besides this, the LCN2-null mice presented a less inflammatory profile in the cerebellum, characterized by decreased expression levels of *Ifn*-gamma, *Il12a* and *Il17a* when compared with the WT animals. Nevertheless, differences between genotypes were only statistically significant for the expression levels of *Ifn-gamma*, during the onset phase of disease. Nam and colleagues (2014) showed similar results for the expression levels of these cytokines in the spinal cord of WT and LCN2-null mice, at day 17 after EAE induction. They also mention that at the chronic phase of disease (day 30 after EAE induction), the expression levels of *Il12* was similar in LCN2-null and WT mice, but they do not show if the expression levels were increased or decreased compared with the levels of day 17. Contrarily, Berard and co-workers (2012) had shown an increase in the expression of *Ifn-gamma* in LCN2-null EAE mice, compared with WT animals, between days 28-32 after EAE induction. However, they compared LCN2-null mice with a chronic disease course with WT animals that developed a relapse-remitting disease, and they had previously shown that WT animals with a chronic disease presented increased expression levels of this cytokine compared with WTs with a relapse-remitting disease (Berard et al., 2010). As for the expression levels of *Il4*, a cytokine produced by Th2 cells, they were not altered by EAE induction, in both genotypes.

To evaluate the percentage of area occupied by inflammatory infiltrates, in the cerebellum, representative sections of the entire cerebellum of EAE animals were stained with luxol fast blue. Both WT and LCN2-null mice presented a decrease in the percentage of lesioned areas in the chronic phase of EAE, compared with the onset phase, similarly to the pattern observed for cytokine gene expression, and again the LCN2-null mice presented a lower percentage of lesion areas, in the onset phase, compared with WT animals, although not statistically significant. Nam and co-workers (2014) studied the presence of inflammatory infiltrates and demyelination not in the cerebellum, but in the spinal cord, and have shown that LCN2-null EAE mice presented less inflammatory infiltrates and less demyelination in the spinal cord, compared with WT EAE animals. In our case, the LCN2-null mice

seem to present less inflammatory infiltrates, but the difference is not statistically significant. In our study, the range of clinical scores at the onset of disease was elevated, ranging from 1.5 to 4, which increased the variability inside the groups at this phase of the disease. Also, they used a qualitative measurement to evaluate the histological score (scale from 0 to 4), and we used a quantitative measure, which involved the delimitation of all lesioned areas per section, in a total of 7 sections per animal, and the normalization for the total white matter. Berard and colleagues (2012) also evaluated lesioned areas in the spinal cord of LCN2-null and WT mice induced with EAE, and found an increase in the total lesioned area per section in the LCN2-null mice when compared with the WT animals. As already mentioned for the gene expression, in this case they also compared LCN2-null animals with a chronic disease course, and WT animals with a relapse-remitting course, while they had previously shown that WT animals with chronic EAE presented an increase in total lesion area, when compared to WT animals with relapse-remitting EAE (Berard et al., 2010). So, the differences found between LCN2-null mice and WT animals could be due to differences in the disease course, and not differences between genotypes. In another study, the total lesion frequency was evaluated in the cerebellum of female C57BL/6 animals induced with MOG_{35-55}, using the HE staining instead of the luxol fast blue. Several timepoints were assessed, during a period of 50 days, and, contrarily to our results, they observed that the number of inflammatory infiltrates was greater at day 16 after EAE induction, and persisted to a similar extent until the end of the experiment. In this study the results were presented as the sum of the total number of meningeal and parenchymal infiltrates (Kuerten et al., 2007), while in our case we measured the total area of inflammatory infiltrates, and normalized the results for the total white matter area. Interestingly, we found a high correlation between the percentage of lesioned area, in the cerebellum, and the clinical score of the animals, while Kuerten and co-workers (2007) did not found a correlation between the clinical score and lesion frequency or lesion size, both in the brain and in the spinal cord of MOG_{35-55}-induced animals.

To further confirm that the delimited lesion areas in the luxol fast blue staining correspond to demyelination areas, we could stain a consecutive section with a myelin marker, like fluoromyelin or an antibody specific for MOG, and check if the areas overlap. Using these stainings, we could also quantify the percentage of demyelination in the cerebellum. It would also be interesting to stain cerebellum sections with OPCs markers, such as NG2 or platelet-derived growth factor receptor (PDGFR)α, and also mature oligodendrocyte markers, like 2',3'-cyclic-nucleotide 3'-phosphodiesterase (CNPase), at both timepoints, to assess if these cells are present near lesion sites, and if they could be involved in the remyelination process.

4.2.4 Astrogliosis in the cerebellum

Previously, it was shown that in the context of a relapse-remitting model of EAE, astrocytes were the only cells producing LCN2, except for infiltrating neutrophils (Marques et al., 2012), so, in order to evaluate the influence of LCN2 in astrocyte morphology and activation, in the cerebellum of EAE mice MOG_{35-55}-induced, we stained cerebellum slices from LCN2-null mice and WT littermates with GFAP, at the onset and chronic phases of EAE. LCN2-null mice and WT littermates non-induced were used as controls. Posteriorly, fluorescence images were taken, from the cerebellar white matter, and were used to quantify the total GFAP+ area with the Fiji software.

Both genotypes presented an elevation in total GFAP+ area, at the onset and chronic phases of disease, when compared to non-induced animals. Previously, the GFAP fluorescence intensity was also quantified, in the spinal cord of LCN2-null and WT mice induced with EAE (Nam et al., 2014). They found a decreased activation of astrocytes in LCN2-null mice compared to WT animals, as assessed by a decrease in the fluorescence intensity. In addition, other studies using LCN2-null mice have shown a decreased GFAP expression, compared to WT animals, after intracerebroventricular injection with LPS (to induce inflammation) or cortical stab wounding (to induce injury) (Lee et al., 2011). In our study we could not find differences between genotypes, but we only have 3 animals per group, so it would be valuable to increase the number of animals. Regarding the expression levels of the *Gfap* gene, they were only elevated during the onset phase of disease, in both genotypes. In this case, for gene expression evaluation, we used the entire cerebellum, including white and grey matter, while the photographs to evaluate the GFAP+ area were only taken in the cerebellar white matter. Also, it is possible that the elevated levels of GFAP protein, resultant from the increase in gene expression during the onset phase, were not cleared by the time the animals reached the chronic phase.

Besides studying the astrocytes, it would also be interesting to evaluate microglial activation in the cerebellum of LCN2-null mice and WT animals, induced with EAE, at both the onset and chronic phases of disease, and if possible microglial morphology.

5. CONCLUDING REMARKS

5. CONCLUDING REMARKS

The role of the thymus in EAE development is extremely important, not only because CD4+ and CD8+ T cells that could become auto-reactive are differentiated in this organ, but also because it is responsible for the production of Treg cells, which try to control the activity of auto-reactive cells. However, few studies have been made to characterize the morphological and functional alterations that occur in the thymus after EAE induction. Even though we have assessed thymocyte populations at two timepoints during disease development, namely the peak of activity of disease and a chronic phase, some questions still remain. Are the thymic populations already altered before the appearance of the first symptoms? Are the corticosterone levels solely responsible for thymic atrophy, in the context of the chronic EAE model? What other factors could also be contributing to thymic atrophy? Does LCN2 influence the production of Treg cells?

Still, the flow cytometry results showing alterations in the proportion of thymic populations, during the onset of EAE, but not during the chronic phase, suggests a role of the thymus in disease establishment, and the better we understand that role, the better we will be able to modulate thymic activity and prevent auto-immune diseases.

Regarding the role of LCN2 in MS disease, so far, two other studies have tried to unravel the role of LCN2 in MS pathogenesis, by using the LCN2-null animals induced with EAE, but these studies have shown contradictory results. The contradictions are mainly related with the clinical outcome of the disease, which is evaluated using a scoring scale highly dependent on the observer. So unless other types of scales are developed, for the evaluation of disease development on EAE, or unless each scale number has a specific and distinct characteristic, facilitating its usability, the comparisons between studies will continue to present difficulties. In addition, the microbiological environment in which the animals live in, i.e., the microbiological status of the animal facilities, is known to affect the immunological state of the animals. Considering that we are studying a protein involved in the acute phase response to inflammatory stimuli, in the context of an auto-immune disease, we should always take into consideration factors that can alter the immunological response in the animals. Apart from this, most EAE studies are performed in female mice, and little is known about the possible influence of the estrous cycle phase in disease development. Recently it was published that EAE induction disrupted the estrous cycle in female SJL/J mice, but is it possible that the appearance of the first symptoms could be influenced by the phase of the cycle at the time of disease induction?

Globally, our results show a similar pattern of response both in the CNS, in the cerebellum, and in the periphery, specifically in the thymus, characterized by increased alterations during the peak of activity of disease, and a re-establishment to normal levels at the chronic phase. In more detail, in the thymus, during the onset phase of disease, the percentage of DP cells is decreased, and the percentages of CD4 and CD8 single positive cells are increased, when compared with non-induced animals. Remarkably, although the total number of cells from each of the thymic populations remained decreased during the chronic phase, the proportions between the different populations were restored. It remains uncertain if the morphology of the thymus is also re-established.

In what concerns the LCN2, and its role in EAE, our results suggest a less inflammatory profile in these animals, characterized by the presence of less inflammatory infiltrates and decreased expression of pro-inflammatory cytokines in the cerebellum. This goes according to previously published data, in which LCN2 was found to play a protective role during EAE development. Still, in our case, the decreased inflammatory profile did not translate into an improvement in the clinical score. So, it would be interesting to also evaluate the spinal cord of our animals, to compare with previous results and try to understand what are the factors that could be contributing for the lack of improvement in the clinical score of our LCN2-null mice induced with EAE.

Although previous work form our group has shown elevated levels of LCN2 in the CSF of MS patients, comparing with healthy-controls, more studies with MS patients should be done to assess if LCN2 could be used as a disease marker, if its' levels were able to distinguish MS from other inflammatory diseases of the CNS, or as a predictor of evolution from CIS to definite MS. Also, longitudinal studies could evaluate the value of LCN2 as a predictive factor of disease progression.

6. REFERENCES

6. REFERENCES

Back, S. A., Tuohy, T. M., Chen, H., Wallingford, N., Craig, A., Struve, J., Luo, N. L., Banine, F., Liu, Y., Chang, A., Trapp, B. D., Bebo, B. F., Jr., Rao, M. S., & Sherman, L. S. (2005). Hyaluronan accumulates in demyelinated lesions and inhibits oligodendrocyte progenitor maturation. *Nature Medicine, 11*(9), 966-972. doi: 10.1038/nm1279

Bao, G., Clifton, M., Hoette, T. M., Mori, K., Deng, S. X., Qiu, A., Viltard, M., Williams, D., Paragas, N., Leete, T., Kulkarni, R., Li, X., Lee, B., Kalandadze, A., Ratner, A. J., Pizarro, J. C., Schmidt-Ott, K. M., Landry, D. W., Raymond, K. N., Strong, R. K., & Barasch, J. (2010). Iron traffics in circulation bound to a siderocalin (Ngal)-catechol complex. *Nature Chemical Biolology, 6*(8), 602-609. doi: 10.1038/nchembio.402

Batoulis, H., Recks, M. S., Addicks, K., & Kuerten, S. (2011). Experimental autoimmune encephalomyelitis–achievements and prospective advances. [Review]. *APMIS, 119*(12), 819-830. doi: 10.1111/j.1600-0463.2011.02794.x

Berard, J. L., Wolak, K., Fournier, S., & David, S. (2010). Characterization of relapsing-remitting and chronic forms of experimental autoimmune encephalomyelitis in C57BL/6 mice. *Glia, 58*(4), 434-445. doi: 10.1002/glia.20935

Berard, J. L., Zarruk, J. G., Arbour, N., Prat, A., Yong, V. W., Jacques, F. H., Akira, S., & David, S. (2012). Lipocalin 2 is a novel immune mediator of experimental autoimmune encephalomyelitis pathogenesis and is modulated in multiple sclerosis. *Glia, 60*(7), 1145-1159. doi: 10.1002/glia.22342

Berge, T., Leikfoss, I. S., & Harbo, H. F. (2013). From Identification to Characterization of the Multiple Sclerosis Susceptibility Gene CLEC16A. *International Journal of Molecular Sciences, 14*(3), 4476-4497. doi: 10.3390/ijms14034476

Billard, M. J., Gruver, A. L., & Sempowski, G. D. (2011). Acute endotoxin-induced thymic atrophy is characterized by intrathymic inflammatory and wound healing responses. *PLoS One, 6*(3), e17940. doi: 10.1371/journal.pone.0017940

Borreani, C., Bianchi, E., Pietrolongo, E., Rossi, I., Cilia, S., Giuntoli, M., Giordano, A., Confalonieri, P., Lugaresi, A., Patti, F., Grasso, M. G., de Carvalho, L. L., Palmisano, L., Zaratin, P., Battaglia, M. A., & Solari, A. (2014). Unmet needs of people with severe multiple sclerosis and their carers: qualitative findings for a home-based intervention. *PLoS One, 9*(10), e109679. doi: 10.1371/journal.pone.0109679

Brambilla, R., Morton, P. D., Ashbaugh, J. J., Karmally, S., Lambertsen, K. L., & Bethea, J. R. (2014). Astrocytes play a key role in EAE pathophysiology by orchestrating in the CNS the inflammatory response of resident and peripheral immune cells and by suppressing remyelination. *Glia, 62*(3), 452-467. doi: 10.1002/glia.22616

Brettschneider, J., Czerwoniak, A., Senel, M., Fang, L., Kassubek, J., Pinkhardt, E., Lauda, F., Kapfer, T., Jesse, S., Lehmensiek, V., Ludolph, A. C., Otto, M., & Tumani, H. (2010). The chemokine CXCL13 is a prognostic marker in clinically isolated syndrome (CIS). *PLoS One, 5*(8), e11986. doi: 10.1371/journal.pone.0011986

Brown, D. A., & Sawchenko, P. E. (2007). Time course and distribution of inflammatory and neurodegenerative events suggest structural bases for the pathogenesis of experimental autoimmune encephalomyelitis. *Journal of Comparative Neurology, 502*(2), 236-260. doi: 10.1002/cne.21307

Chandran, S., Hunt, D., Joannides, A., Zhao, C., Compston, A., & Franklin, R. J. (2008). Myelin repair: the role of stem and precursor cells in multiple sclerosis. [Review]. *Philosophical Transactions of the Royal Society of London. Series B, Biological Sciences, 363*(1489), 171-183. doi: 10.1098/rstb.2006.2019

Chari, D. M., & Blakemore, W. F. (2002). New insights into remyelination failure in multiple sclerosis: implications for glial cell transplantation. [Review]. *Multiple Sclerosis, 8*(4), 271-277.

Chen, X., Fang, L., Song, S., Guo, T. B., Liu, A., & Zhang, J. Z. (2009). Thymic regulation of autoimmune disease by accelerated differentiation of Foxp3+ regulatory T cells through IL-7 signaling pathway. *Journal of Immunology, 183*(10), 6135-6144. doi: 10.4049/jimmunol.0901576

Chia, W. J., Dawe, G. S., & Ong, W. Y. (2011). Expression and localization of the iron-siderophore binding protein lipocalin 2 in the normal rat brain and after kainate-induced excitotoxicity. *Neurochemistry International, 59*(5), 591-599. doi: 10.1016/j.neuint.2011.04.007

Choi, J., Lee, H. W., & Suk, K. (2011). Increased plasma levels of lipocalin 2 in mild cognitive impairment. [Clinical Trial, Comparative Study]. *Journal of the Neurological Sciences, 305*(1-2), 28-33. doi: 10.1016/j.jns.2011.03.023

Comi, G., Colombo, B., & Martinelli, V. (2000). Prognosis-modifying therapy in multiple sclerosis. [Review]. *Neurological Sciences, 21*(4 Suppl 2), S893-899.

Compston, A., & Coles, A. (2008). Multiple sclerosis. *Lancet, 372*(9648), 1502-1517. doi: 10.1016/S0140-6736(08)61620-7

Constantinescu, C. S., Farooqi, N., O'Brien, K., & Gran, B. (2011). Experimental autoimmune encephalomyelitis (EAE) as a model for multiple sclerosis (MS). [Review]. *British Journal of Pharmacology, 164*(4), 1079-1106. doi: 10.1111/j.1476-5381.2011.01302.x

Correale, J. (2014). The role of microglial activation in disease progression. *Multiple Sclerosis, 20*(10), 1288-1295. doi: 10.1177/1352458514533230

Croxford, A. L., Kurschus, F. C., & Waisman, A. (2011). Mouse models for multiple sclerosis: historical facts and future implications. [Review]. *Biochimica et Biophysica Acta, 1812*(2), 177-183. doi: 10.1016/j.bbadis.2010.06.010

Dal Canto, M. C., Melvold, R. W., Kim, B. S., & Miller, S. D. (1995). Two models of multiple sclerosis: experimental allergic encephalomyelitis (EAE) and Theiler's murine encephalomyelitis virus (TMEV) infection. A pathological and immunological comparison. [Review]. *Microscopy Research and Technique, 32*(3), 215-229. doi: 10.1002/jemt.1070320305

de la Rosa, P., Barnett, J. B., & Schafer, R. (2005). Characterization of thymic atrophy and the mechanism of thymocyte depletion after in vivo exposure to a mixture of herbicides. *Journal of Toxicology and Environmental Health, 68*(2), 81-98. doi: 10.1080/15287390590886072

Denic, A., Johnson, A. J., Bieber, A. J., Warrington, A. E., Rodriguez, M., & Pirko, I. (2011). The relevance of animal models in multiple sclerosis research. *Pathophysiology, 18*(1), 21-29. doi: 10.1016/j.pathophys.2010.04.004

Devireddy, L. R., Gazin, C., Zhu, X., & Green, M. R. (2005). A cell-surface receptor for lipocalin 24p3 selectively mediates apoptosis and iron uptake. *Cell, 123*(7), 1293-1305. doi: 10.1016/j.cell.2005.10.027

Devireddy, L. R., Hart, D. O., Goetz, D. H., & Green, M. R. (2010). A mammalian siderophore synthesized by an enzyme with a bacterial homolog involved in enterobactin production. *Cell, 141*(6), 1006-1017. doi: 10.1016/j.cell.2010.04.040

di Penta, A., Moreno, B., Reix, S., Fernandez-Diez, B., Villanueva, M., Errea, O., Escala, N., Vandenbroeck, K., Comella, J. X., & Villoslada, P. (2013). Oxidative stress and proinflammatory cytokines contribute to demyelination and axonal damage in a cerebellar culture model of neuroinflammation. *PLoS One, 8*(2), e54722. doi: 10.1371/journal.pone.0054722

Djikic, J., Nacka-Aleksic, M., Pilipovic, I., Kosec, D., Arsenovic-Ranin, N., Stojic-Vukanic, Z., Dimitrijevic, M., & Leposavic, G. (2015). Age-related changes in spleen of Dark Agouti rats immunized for experimental autoimmune encephalomyelitis. *Journal of Neuroimmunology, 278*, 123-135. doi: 10.1016/j.jneuroim.2014.12.014

Duszczyszyn, D. A., Williams, J. L., Mason, H., Lapierre, Y., Antel, J., & Haegert, D. G. (2010). Thymic involution and proliferative T-cell responses in multiple sclerosis. *Journal of Neuroimmunology, 221*(1-2), 73-80. doi: 10.1016/j.jneuroim.2010.02.005

Ebers, G. C. (2008). Environmental factors and multiple sclerosis. [Review]. *Lancet Neurology, 7*(3), 268-277. doi: 10.1016/S1474-4422(08)70042-5

Ferreira, A. C., Pinto, V., Da Mesquita, S., Novais, A., Sousa, J. C., Correia-Neves, M., Sousa, N., Palha, J. A., & Marques, F. (2013). Lipocalin-2 is involved in emotional behaviors and cognitive function. *Frontiers in Cellullar Neuroscience, 7*, 122. doi: 10.3389/fncel.2013.00122

Flechter, S., Vardi, J., Just, I., Arnon, R., & Teitelbaum, D. (1984). Thymectomy and chronic relapsing experimental allergic encephalomyelitis in guinea pigs. *Archives of Neurology, 41*(11), 1158-1160.

Flo, T. H., Smith, K. D., Sato, S., Rodriguez, D. J., Holmes, M. A., Strong, R. K., Akira, S., & Aderem, A. (2004). Lipocalin 2 mediates an innate immune response to bacterial infection by sequestrating iron. *Nature, 432*(7019), 917-921. doi: 10.1038/nature03104

Flower, D. R. (1996). The lipocalin protein family: structure and function. [Review]. *Biochemical Journal, 318 (Pt 1)*, 1-14.

Fossey, S. C., Vnencak-Jones, C. L., Olsen, N. J., Sriram, S., Garrison, G., Deng, X., Crooke, P. S., 3rd, & Aune, T. M. (2007). Identification of molecular biomarkers for multiple sclerosis. *Journal of Molecular Diagnostics, 9*(2), 197-204. doi: 10.2353/jmoldx.2007.060147

Franklin, R. J. (2002). Why does remyelination fail in multiple sclerosis? [Review]. *Nature Reviews Neuroscience, 3*(9), 705-714. doi: 10.1038/nrn917

Frohman, E. M., Racke, M. K., & Raine, C. S. (2006). Multiple sclerosis–the plaque and its pathogenesis. [Review]. *New England Journal of Medicine, 354*(9), 942-955. doi: 10.1056/NEJMra052130

Goetz, D. H., Holmes, M. A., Borregaard, N., Bluhm, M. E., Raymond, K. N., & Strong, R. K. (2002). The neutrophil lipocalin NGAL is a bacteriostatic agent that interferes with siderophore-mediated iron acquisition. *Molecular Cell, 10*(5), 1033-1043.

Goldrath, A. W., & Bevan, M. J. (1999). Selecting and maintaining a diverse T-cell repertoire. [Review]. *Nature, 402*(6759), 255-262. doi: 10.1038/46218

Gran, B., Yu, S., Zhang, G. X., & Rostami, A. (2010). Accelerated thymocyte maturation in IL-12Rbeta2-deficient mice contributes to increased susceptibility to autoimmune inflammatory demyelination. *Experimental and Molecular Pathology, 89*(2), 126-134. doi: 10.1016/j.yexmp.2010.06.003

Gruver, A. L., & Sempowski, G. D. (2008). Cytokines, leptin, and stress-induced thymic atrophy. [Review]. *Journal of Leukocyte Biolology, 84*(4), 915-923. doi: 10.1189/jlb.0108025

Guo, X., Nakamura, K., Kohyama, K., Harada, C., Behanna, H. A., Watterson, D. M., Matsumoto, Y., & Harada, T. (2007). Inhibition of glial cell activation ameliorates the severity of experimental autoimmune encephalomyelitis. *Neuroscience Research, 59*(4), 457-466. doi: 10.1016/j.neures.2007.08.014

Hafler, D. A., Compston, A., Sawcer, S., Lander, E. S., Daly, M. J., De Jager, P. L., de Bakker, P. I., Gabriel, S. B., Mirel, D. B., Ivinson, A. J., Pericak-Vance, M. A., Gregory, S. G., Rioux, J. D., McCauley, J. L., Haines, J. L., Barcellos, L. F., Cree, B., Oksenberg, J. R., & Hauser, S. L. (2007). Risk alleles for multiple sclerosis identified by a genomewide study. *New England Journal of Medicine, 357*(9), 851-862. doi: 10.1056/NEJMoa073493

Hafler, D. A., Slavik, J. M., Anderson, D. E., O'Connor, K. C., De Jager, P., & Baecher-Allan, C. (2005). Multiple sclerosis. [Review]. *Immunological Reviews, 204*, 208-231. doi: 10.1111/j.0105-2896.2005.00240.x

Handel, A. E., Lincoln, M. R., & Ramagopalan, S. V. (2011). Of mice and men: experimental autoimmune encephalitis and multiple sclerosis. [Review]. *European Journal of Clinical Investigation, 41*(11), 1254-1258. doi: 10.1111/j.1365-2362.2011.02519.x

Hara, N., Yoshida, S., Takai, N., Saito, T., & Tanaka, R. (1986). [Morphological changes of the thymus and spleen with acute experimental allergic encephalomyelitis (EAE) in Lewis rats]. *No To Shinkei, 38*(1), 81-85.

Hirahara, H., Ogawa, M., Kimura, M., Iiai, T., Tsuchida, M., Hanawa, H., Watanabe, H., & Abo, T. (1994). Glucocorticoid independence of acute thymic involution induced by lymphotoxin and estrogen. *Cellular Immunology, 153*(2), 401-411. doi: 10.1006/cimm.1994.1038

Hisahara, S., Yuan, J., Momoi, T., Okano, H., & Miura, M. (2001). Caspase-11 mediates oligodendrocyte cell death and pathogenesis of autoimmune-mediated demyelination. *Journal of Experimental Medicine, 193*(1), 111-122.

Howard, J. K., Lord, G. M., Matarese, G., Vendetti, S., Ghatei, M. A., Ritter, M. A., Lechler, R. I., & Bloom, S. R. (1999). Leptin protects mice from starvation-induced lymphoid atrophy and increases thymic cellularity in ob/ob mice. *Journal of Clinical Investigation, 104*(8), 1051-1059. doi: 10.1172/JCI6762

Ip, J. P., Nocon, A. L., Hofer, M. J., Lim, S. L., Muller, M., & Campbell, I. L. (2011). Lipocalin 2 in the central nervous system host response to systemic lipopolysaccharide administration. *Journal of Neuroinflammation, 8*, 124. doi: 10.1186/1742-2094-8-124

Jang, E., Kim, J. H., Lee, S., Seo, J. W., Jin, M., Lee, M. G., Jang, I. S., Lee, W. H., & Suk, K. (2013). Phenotypic polarization of activated astrocytes: the critical role of lipocalin-2 in the classical inflammatory activation of astrocytes. *Journal of Immunology, 191*(10), 5204-5219. doi: 10.4049/jimmunol.1301637

Jha, M. K., Jeon, S., Jin, M., Ock, J., Kim, J. H., Lee, W. H., & Suk, K. (2014). The pivotal role played by lipocalin-2 in chronic inflammatory pain. *Experimental Neurology, 254*, 41-53. doi: 10.1016/j.expneurol.2014.01.009

Joy, J. E., & Johnston Jr., R. B. (2001). *Multiple sclerosis - Current status and strategies for the future.* Washington, DC: National Academy of Sciences.

Kjeldsen, L., Bainton, D. F., Sengelov, H., & Borregaard, N. (1993). Structural and functional heterogeneity among peroxidase-negative granules in human neutrophils: identification of a distinct gelatinase-containing granule subset by combined immunocytochemistry and subcellular fractionation. *Blood, 82*(10), 3183-3191.

Kjeldsen, L., Bainton, D. F., Sengelov, H., & Borregaard, N. (1994). Identification of neutrophil gelatinase-associated lipocalin as a novel matrix protein of specific granules in human neutrophils. *Blood, 83*(3), 799-807.

Kothavale, A., Di Gregorio, D., Somera, F. P., & Smith, M. E. (1995). GFAP mRNA fluctuates in synchrony with chronic relapsing EAE symptoms in SJL/J mice. *Glia, 14*(3), 216-224. doi: 10.1002/glia.440140307

Kuerten, S., Kostova-Bales, D. A., Frenzel, L. P., Tigno, J. T., Tary-Lehmann, M., Angelov, D. N., & Lehmann, P. V. (2007). MP4- and MOG:35-55-induced EAE in C57BL/6 mice differentially targets brain, spinal cord and cerebellum. *Journal of Neuroimmunology, 189*(1-2), 31-40. doi: 10.1016/j.jneuroim.2007.06.016

Kuerten, S., & Lehmann, P. V. (2011). The immune pathogenesis of experimental autoimmune encephalomyelitis: lessons learned for multiple sclerosis? [Review]. *Journal of Interferon and Cytokine Research, 31*(12), 907-916. doi: 10.1089/jir.2011.0072

Lassmann, H., & van Horssen, J. (2011). The molecular basis of neurodegeneration in multiple sclerosis. [Review]. *FEBS Letters, 585*(23), 3715-3723. doi: 10.1016/j.febslet.2011.08.004

Lee, S., Kim, J. H., Seo, J. W., Han, H. S., Lee, W. H., Mori, K., Nakao, K., Barasch, J., & Suk, K. (2011). Lipocalin-2 Is a chemokine inducer in the central nervous system: role of chemokine ligand 10 (CXCL10) in lipocalin-2-induced cell migration. *Journal of Biological Chemistry, 286*(51), 43855-43870. doi: 10.1074/jbc.M111.299248

Lee, S., Lee, J., Kim, S., Park, J. Y., Lee, W. H., Mori, K., Kim, S. H., Kim, I. K., & Suk, K. (2007). A dual role of lipocalin 2 in the apoptosis and deramification of activated microglia. *Journal of Immunology, 179*(5), 3231-3241.

Lee, S., Park, J. Y., Lee, W. H., Kim, H., Park, H. C., Mori, K., & Suk, K. (2009). Lipocalin-2 is an autocrine mediator of reactive astrocytosis. *Journal of Neuroscience, 29*(1), 234-249. doi: 10.1523/JNEUROSCI.5273-08.2009

Liedtke, W., Edelmann, W., Chiu, F. C., Kucherlapati, R., & Raine, C. S. (1998). Experimental autoimmune encephalomyelitis in mice lacking glial fibrillary acidic protein is characterized by a more severe clinical course and an infiltrative central nervous system lesion. *American Journal of Pathology, 152*(1), 251-259.

Litwak, S. A., Payne, N. L., Campanale, N., Ozturk, E., Lee, J. Y., Petratos, S., Siatskas, C., Bakhuraysah, M., & Bernard, C. C. (2013). Nogo-receptor 1 deficiency has no influence on immune cell repertoire or function during experimental autoimmune encephalomyelitis. *PLoS One, 8*(12), e82101. doi: 10.1371/journal.pone.0082101

Liu, H., MacKenzie-Graham, A. J., Kim, S., & Voskuhl, R. R. (2001). Mice resistant to experimental autoimmune encephalomyelitis have increased thymic expression of myelin basic protein and increased MBP specific T cell tolerance. *Journal of Neuroimmunology, 115*(1-2), 118-126.

Liu, Q., & Nilsen-Hamilton, M. (1995). Identification of a new acute phase protein. [Comparative Study]. *Journal of Biological Chemistry, 270*(38), 22565-22570.

Lucchinetti, C. F., Parisi, J., & Bruck, W. (2005). The pathology of multiple sclerosis. [Review]. *Neurologic Clinics, 23*(1), 77-105, vi. doi: 10.1016/j.ncl.2004.09.002

MacKenzie-Graham, A., Tinsley, M. R., Shah, K. P., Aguilar, C., Strickland, L. V., Boline, J., Martin, M., Morales, L., Shattuck, D. W., Jacobs, R. E., Voskuhl, R. R., & Toga, A. W. (2006). Cerebellar cortical atrophy in experimental autoimmune encephalomyelitis. *Neuroimage, 32*(3), 1016-1023. doi: 10.1016/j.neuroimage.2006.05.006

MacKenzie-Graham, A., Tiwari-Woodruff, S. K., Sharma, G., Aguilar, C., Vo, K. T., Strickland, L. V., Morales, L., Fubara, B., Martin, M., Jacobs, R. E., Johnson, G. A., Toga, A. W., & Voskuhl, R. R. (2009). Purkinje cell loss in experimental autoimmune encephalomyelitis. *Neuroimage, 48*(4), 637-651. doi: 10.1016/j.neuroimage.2009.06.073

MacPhee, I. A., Antoni, F. A., & Mason, D. W. (1989). Spontaneous recovery of rats from experimental allergic encephalomyelitis is dependent on regulation of the immune system by endogenous adrenal corticosteroids. *Journal of Experimental Medicine, 169*(2), 431-445.

Marques, F., Mesquita, S. D., Sousa, J. C., Coppola, G., Gao, F., Geschwind, D. H., Columba-Cabezas, S., Aloisi, F., Degn, M., Cerqueira, J. J., Sousa, N., Correia-Neves, M., & Palha, J. A. (2012). Lipocalin 2 is present in the EAE brain and is modulated by natalizumab. *Frontiers in Cellular Neuroscience, 6*, 33. doi: 10.3389/fncel.2012.00033

Marques, F., Rodrigues, A. J., Sousa, J. C., Coppola, G., Geschwind, D. H., Sousa, N., Correia-Neves, M., & Palha, J. A. (2008). Lipocalin 2 is a choroid plexus acute-phase protein. *Journal of Cerebral Blood Flow and Metabolism, 28*(3), 450-455. doi: 10.1038/sj.jcbfm.9600557

Matejuk, A., Hopke, C., Vandenbark, A. A., Hurn, P. D., & Offner, H. (2005). Middle-age male mice have increased severity of experimental autoimmune encephalomyelitis and are unresponsive to testosterone therapy. [Comparative Study]. *Journal of Immunology, 174*(4), 2387-2395.

Mesquita, S. D., Ferreira, A. C., Falcao, A. M., Sousa, J. C., Oliveira, T. G., Correia-Neves, M., Sousa, N., Marques, F., & Palha, J. A. (2014). Lipocalin 2 modulates the cellular response to amyloid beta. *Cell Death and Differentiation, 21*(10), 1588-1599. doi: 10.1038/cdd.2014.68

Michie, A. M., & Zuniga-Pflucker, J. C. (2002). Regulation of thymocyte differentiation: pre-TCR signals and beta-selection. [Review]. *Seminars in Immunology, 14*(5), 311-323.

Miller, E. (2012). Multiple sclerosis. [Review]. *Advances in Experimental Medicine and Biology, 724*, 222-238. doi: 10.1007/978-1-4614-0653-2_17

Minagar, A., Shapshak, P., Fujimura, R., Ownby, R., Heyes, M., & Eisdorfer, C. (2002). The role of macrophage/microglia and astrocytes in the pathogenesis of three neurologic disorders: HIV-associated dementia, Alzheimer disease, and multiple sclerosis. [Review]. *Journal of the Neurological Sciences, 202*(1-2), 13-23.

Mix, E., Meyer-Rienecker, H., Hartung, H. P., & Zettl, U. K. (2010). Animal models of multiple sclerosis–potentials and limitations. [Historical Article, Review]. *Progress in Neurobiology, 92*(3), 386-404. doi: 10.1016/j.pneurobio.2010.06.005

Murphy, A. C., Lalor, S. J., Lynch, M. A., & Mills, K. H. (2010). Infiltration of Th1 and Th17 cells and activation of microglia in the CNS during the course of experimental autoimmune encephalomyelitis. *Brain, Behaviour and Immunity, 24*(4), 641-651. doi: 10.1016/j.bbi.2010.01.014

Nair, A., Frederick, T. J., & Miller, S. D. (2008). Astrocytes in multiple sclerosis: a product of their environment. [Review]. *Cellular and Molecular Life Sciences, 65*(17), 2702-2720. doi: 10.1007/s00018-008-8059-5

Nakahara, J., Aiso, S., & Suzuki, N. (2010). Autoimmune versus oligodendrogliopathy: the pathogenesis of multiple sclerosis. [Review]. *Archivum Immunologiae et Therapia Experimentalis, 58*(5), 325-333. doi: 10.1007/s00005-010-0094-x

Nakanishi, H. (2003). Microglial functions and proteases. [Review]. *Molecular Neurobiology, 27*(2), 163-176. doi: 10.1385/MN:27:2:163

Nam, Y., Kim, J. H., Seo, M., Jin, M., Jeon, S., Seo, J. W., Lee, W. H., Bing, S. J., Jee, Y., Lee, W. K., Park, D. H., Kook, H., & Suk, K. (2014). Lipocalin-2 protein deficiency ameliorates experimental autoimmune encephalomyelitis: the pathogenic role of lipocalin-2 in the central nervous system and peripheral lymphoid tissues. *Journal of Biological Chemistry, 289*(24), 16773-16789. doi: 10.1074/jbc.M113.542282

Napoli, I., & Neumann, H. (2010). Protective effects of microglia in multiple sclerosis. [Review]. *Experimental Neurology, 225*(1), 24-28. doi: 10.1016/j.expneurol.2009.04.024

Naude, P. J., Nyakas, C., Eiden, L. E., Ait-Ali, D., van der Heide, R., Engelborghs, S., Luiten, P. G., De Deyn, P. P., den Boer, J. A., & Eisel, U. L. (2012). Lipocalin 2: novel component of proinflammatory signaling in Alzheimer's disease. *FASEB Journal, 26*(7), 2811-2823. doi: 10.1096/fj.11-202457

Noseworthy, J. H., Lucchinetti, C., Rodriguez, M., & Weinshenker, B. G. (2000). Multiple sclerosis. [Review]. *New England Journal of Medicine, 343*(13), 938-952. doi: 10.1056/NEJM200009283431307

Nylander, A., & Hafler, D. A. (2012). Multiple sclerosis. [Review]. *Journal of Clinical Investigation, 122*(4), 1180-1188. doi: 10.1172/JCI58649

Pearse, G. (2006). Normal structure, function and histology of the thymus. [Review]. *Toxicologic Pathology, 34*(5), 504-514. doi: 10.1080/01926230600865549

Polman, C. H., Reingold, S. C., Banwell, B., Clanet, M., Cohen, J. A., Filippi, M., Fujihara, K., Havrdova, E., Hutchinson, M., Kappos, L., Lublin, F. D., Montalban, X., O'Connor, P., Sandberg-Wollheim, M., Thompson, A. J., Waubant, E., Weinshenker, B., & Wolinsky, J. S. (2011). Diagnostic criteria for multiple sclerosis: 2010 revisions to the McDonald criteria. *Annals of Neurology, 69*(2), 292-302. doi: 10.1002/ana.22366

Procaccini, C., De Rosa, V., Pucino, V., Formisano, L., & Matarese, G. (2015). Animal models of Multiple Sclerosis. *European Journal of Pharmacology*. doi: 10.1016/j.ejphar.2015.03.042

Purves, D., Augustine, G. J., Fitzpatrick, D., Katz, L. C., LaMantia, A.-S., McNamara, J. O., & Williams, S. M. (2001). *Neuroscience* (Second ed.). Sunderland (MA): Sinauer Associates, Inc.

Ramaglia, V., Jackson, S. J., Hughes, T. R., Neal, J. W., Baker, D., & Morgan, B. P. (2015). Complement activation and expression during chronic relapsing experimental autoimmune encephalomyelitis in the Biozzi ABH mouse. *Clinical and Experimental Immunology*. doi: 10.1111/cei.12595

Ransohoff, R. M. (2012). Animal models of multiple sclerosis: the good, the bad and the bottom line. *Nature Neuroscience, 15*(8), 1074-1077. doi: 10.1038/nn.3168

Rathore, K. I., Berard, J. L., Redensek, A., Chierzi, S., Lopez-Vales, R., Santos, M., Akira, S., & David, S. (2011). Lipocalin 2 plays an immunomodulatory role and has detrimental effects after spinal cord injury. *Journal of Neuroscience, 31*(38), 13412-13419. doi: 10.1523/JNEUROSCI.0116-11.2011

Reboldi, A., Coisne, C., Baumjohann, D., Benvenuto, F., Bottinelli, D., Lira, S., Uccelli, A., Lanzavecchia, A., Engelhardt, B., & Sallusto, F. (2009). C-C chemokine receptor 6-regulated entry of TH-17 cells into the CNS through the choroid plexus is required for the initiation of EAE. *Nature Immunology, 10*(5), 514-523. doi: 10.1038/ni.1716

Reynolds, R., Dawson, M., Papadopoulos, D., Polito, A., Di Bello, I. C., Pham-Dinh, D., & Levine, J. (2002). The response of NG2-expressing oligodendrocyte progenitors to demyelination in MOG-EAE and MS. *Journal of Neurocytology, 31*(6-7), 523-536.

Rivers, T. M., Sprunt, D. H., & Berry, G. P. (1933). Observations on Attempts to Produce Acute Disseminated Encephalomyelitis in Monkeys. *Journal of Experimental Medicine, 58*(1), 39-53.

Rose, N. R. (1994). Thymus function, ageing and autoimmunity. [Review]. *Immunology Letters, 40*(3), 225-230.

Savage, P. A., & Davis, M. M. (2001). A kinetic window constricts the T cell receptor repertoire in the thymus. *Immunity, 14*(3), 243-252.

Sawcer, S., Franklin, R. J., & Ban, M. (2014). Multiple sclerosis genetics. *Lancet Neurology, 13*(7), 700-709. doi: 10.1016/S1474-4422(14)70041-9

Schindelin, J., Arganda-Carreras, I., Frise, E., Kaynig, V., Longair, M., Pietzsch, T., Preibisch, S., Rueden, C., Saalfeld, S., Schmid, B., Tinevez, J. Y., White, D. J., Hartenstein, V., Eliceiri, K., Tomancak, P., & Cardona, A. (2012). Fiji: an open-source platform for biological-image analysis. *Nature Methods, 9*(7), 676-682. doi: 10.1038/nmeth.2019

Schuurman, H. J., Kuper, C. F., & Kendall, M. D. (1997). Thymic microenvironment at the light microscopic level. *Microscopy Research and Technique, 38*(3), 216-226. doi: 10.1002/(SICI)1097-0029(19970801)38:3<216::AID-JEMT3>3.0.CO;2-K

Shashidharamurthy, R., Machiah, D., Aitken, J. D., Putty, K., Srinivasan, G., Chassaing, B., Parkos, C. A., Selvaraj, P., & Vijay-Kumar, M. (2013). Differential role of lipocalin 2 during immune complex-mediated acute and chronic inflammation in mice. *Arthritis and Rheumatology, 65*(4), 1064-1073. doi: 10.1002/art.37840

Siatskas, C., Seach, N., Sun, G., Emerson-Webber, A., Silvain, A., Toh, B. H., Alderuccio, F., Backstrom, B. T., Boyd, R. L., & Bernard, C. C. (2012). Thymic gene transfer of myelin oligodendrocyte glycoprotein ameliorates the onset but not the progression of autoimmune demyelination. *Molecular Therapy, 20*(7), 1349-1359. doi: 10.1038/mt.2012.15

Slavin, A., Ewing, C., Liu, J., Ichikawa, M., Slavin, J., & Bernard, C. C. (1998). Induction of a multiple sclerosis-like disease in mice with an immunodominant epitope of myelin oligodendrocyte glycoprotein. *Autoimmunity, 28*(2), 109-120.

Slavin, A., Kelly-Modis, L., Labadia, M., Ryan, K., & Brown, M. L. (2010). Pathogenic mechanisms and experimental models of multiple sclerosis. [Review]. *Autoimmunity, 43*(7), 504-513. doi: 10.3109/08916931003674733

Smith, M. E., Somera, F. P., & Eng, L. F. (1983). Immunocytochemical staining for glial fibrillary acidic protein and the metabolism of cytoskeletal proteins in experimental allergic encephalomyelitis. *Brain Research, 264*(2), 241-253.

Sofroniew, M. V. (2005). Reactive astrocytes in neural repair and protection. [Review]. *Neuroscientist: a review journal bringing neurobiology, neurology and psychiatry, 11*(5), 400-407. doi: 10.1177/1073858405278321

Song, F., Guan, Z., Gienapp, I. E., Shawler, T., Benson, J., & Whitacre, C. C. (2006). The thymus plays a role in oral tolerance in experimental autoimmune encephalomyelitis. *Journal of Immunology, 177*(3), 1500-1509.

Sospedra, M., & Martin, R. (2005). Immunology of multiple sclerosis. [Review]. *Annual Review of Immunology, 23*, 683-747. doi: 10.1146/annurev.immunol.23.021704.115707

Steinman, L. (2001). Multiple sclerosis: a two-stage disease. [News]. *Nature Immunology, 2*(9), 762-764. doi: 10.1038/ni0901-762

Stromnes, I. M., & Goverman, J. M. (2006). Active induction of experimental allergic encephalomyelitis. *Nature Protocols, 1*(4), 1810-1819. doi: 10.1038/nprot.2006.285

Swanborg, R. H. (1995). Experimental autoimmune encephalomyelitis in rodents as a model for human demyelinating disease. [Review]. *Clinical of Immunology and Immunopathology, 77*(1), 4-13.

Takahama, Y. (2006). Journey through the thymus: stromal guides for T-cell development and selection. [Review]. *Nature Reviews Immunology, 6*(2), 127-135. doi: 10.1038/nri1781

Vartanian, T., Li, Y., Zhao, M., & Stefansson, K. (1995). Interferon-gamma-induced oligodendrocyte cell death: implications for the pathogenesis of multiple sclerosis. *Molecular Medicine, 1*(7), 732-743.

Weinshenker, B. G., Issa, M., & Baskerville, J. (1996). Long-term and short-term outcome of multiple sclerosis: a 3-year follow-up study. *Archives of Neurology, 53*(4), 353-358.

Wekerle, H., & Kurschus, F. C. (2006). Animal models of multiple sclerosis. *Drug Discovery Today Disease Models, 3*(4), 359-367. doi: 10.1016/j.ddmod.2006.11.004

Wekerle, H., & Linington, C. (2006). Organ specific autoantigens and the autoreactiveT cell repertoire: the case of myelin oligodendrocyte glycoprotein. [Comment]. *European Journal of Immunology, 36*(3), 512-515. doi: 10.1002/eji.200635914

Williams, A., Piaton, G., & Lubetzki, C. (2007). Astrocytes–friends or foes in multiple sclerosis? *Glia, 55*(13), 1300-1312. doi: 10.1002/glia.20546

Woodruff, R. H., & Franklin, R. J. (1999). Demyelination and remyelination of the caudal cerebellar peduncle of adult rats following stereotaxic injections of lysolecithin, ethidium bromide, and complement/anti-galactocerebroside: a comparative study. *Glia, 25*(3), 216-228.

Yang, J., Goetz, D., Li, J. Y., Wang, W., Mori, K., Setlik, D., Du, T., Erdjument-Bromage, H., Tempst, P., Strong, R., & Barasch, J. (2002). An iron delivery pathway mediated by a lipocalin. *Molecular Cell, 10*(5), 1045-1056.

Zelenay, S., Bergman, M. L., Paiva, R. S., Lino, A. C., Martins, A. C., Duarte, J. H., Moraes-Fontes, M. F., Bilate, A. M., Lafaille, J. J., & Demengeot, J. (2010). Cutting edge: Intrathymic differentiation of adaptive Foxp3+ regulatory T cells upon peripheral proinflammatory immunization. *Journal of Immunology, 185*(7), 3829-3833. doi: 10.4049/jimmunol.1001281

Zuniga-Pflucker, J. C., & Lenardo, M. J. (1996). Regulation of thymocyte development from immature progenitors. [Review]. *Current Opinion in Immunology, 8*(2), 215-224.

ANNEX I – DNA SEQUENCES OF THE PRIMERS USED IN QRT-PCR

Mouse cDNAs	Primer sequences	GenBank™ accession number	Annealing temperature/°C
Hprt	Forward: 5' GCT GGT GAA AAG GAC CTC T 3' Reverse: 5' CAC AGG ACT AGA ACA CCT GC 3'	NM_013556.2	59
Il-17a	Forward: 5' GGA CTC TCC ACC GCA ATG AA 3' Reverse: 5' CAT GTG GTG GTC CAG CTT TC 3'	NM_010552.3	59
Il-12a	Forward: 5' GTG TCT TAG CCA GTC CCG AA 3' Reverse: 5' TTC AAG TCC TCA TAG ATG CTA CCA A 3'	NM_008351.3	59
Il-4	Forward: 5' GTC ACA GGA GAA GGG ACG CCA T 3' Reverse: 5' AGC CCT ACA GAC GAG CTC ACT C 3'	NM_021283.2	59
Inf-γ	Forward: 5' CAA CAG CAA GGC GAA AAA GG 3' Reverse: 5' GGA CCA CTC GGA TGA GCT CA 3'	NM_008337.3	59
Gfap	Forward: 5' AAA CCG CAT CAC CAT TCC TG 3' Reverse: 5' TCT GGT GAG CCT GTA TTG GG 3'	XR_388347.2	59